UNIVERSITY OF LEEDS

This is a repository copy of *Smart frequency control in low inertia energy systems based on frequency response techniques: A review*.

White Rose Research Online URL for this paper:
https://eprints.whiterose.ac.uk/164890/

Version: Accepted Version

White Rose
university consortium
Universities of Leeds, Sheffield & York

eprints@whiterose.ac.uk
https://eprints.whiterose.ac.uk/

Smart frequency control in low inertia energy systems based on frequency response techniques: A review

Yi Cheng[1], Rasoul Azizipanah-Abarghooee[2], Sadegh Azizi[3], Lei Ding[4], Vladimir Terzija[1,*]

[1] School of Electrical and Electronic Engineering, The University of Manchester, Manchester, England, UK
[2] National Grid ESO, CV346DA Warwick, U.K.
[3] School of Electronic and Electrical Engineering, University of Leeds, Leeds, UK
[4] Shandong University, No.17923, Jingshi Road, Jinan, People's Republic of China
[*] vladimir.terzija@manchester.ac.uk

Highlights:

- Classification of frequency response techniques rigorously discussed.
- Advantages and disadvantages of frequency support approaches presented.
- Effects of secondary frequency dips on the system response addressed.
- Frequency control in integrated energy systems elaborated.
- New research and applications related directions are addressed.

Abstract:
Integrated energy systems are considered as an indispensable part of the pathway towards a low-carbon sustainable future, as well as secure and reliable systems, characterised with a high level of flexibility and resilience. Increased penetration of renewable energy sources into energy systems is contributing to the reduction of carbon emission, thereby reducing the level or air pollution, climate changes and supporting the quality of life on the Earth. In this context, energy conversion systems realized by wind turbine generators have been and are still in the focus of extensive research on different system aspects, from planning, exploitation, monitoring, control, or protection perspective. To maximize the utilisation of available wind energy, modern wind turbine generators are connected to the main grid over power electronics (e.g. Type-3, or Type-4 wind generators). Consequently, they are electromagnetically disconnected from the rest of the power system and they provide little or no inertia, contrary to conventional synchronous generators, synchronously connected to the grid and synchronously operated to each other. This synchronism is necessary to ensure a stable system operation. The reduction of the system inertia imposes serious technical challenges on preserving system frequency stability. As it is known, inertia is one of key factors determining the robustness of power systems against sudden active power imbalances caused by different types of frequency events (generator disconnection, or load connection). The reduction of synchronous power reserves further intensifies this problem by reducing the system ability to maintain frequency within a permissible range following frequency events. Consequently, grid operators demand renewable energy sources, which are also referred to as nonsynchronous generators, to emulate the behaviour of synchronous generators to some extent and to participate in (fast) frequency control upon need. In general, countermeasures applied to these sources to contribute to frequency support are classified into two main categories: a) temporary and b) persistent energy reserve-based approaches. This paper presents a review on latest research findings and developed mechanisms for frequency control using wind energy conversion systems as the most frequently deployed renewable energy sources in modern power systems. Relying on lessons learned from the past two decades, in this paper current and future challenges, feasible solutions and subsequent research prospects are detailed. Some key principles that should underlie future changes of wind integrated energy systems are suggested and further research directions are addressed.

Keywords:
Frequency response techniques
Frequency stability challenges
Integrated energy systems
Kinetic energy reserves
Power system inertia
Review
Wind energy conversion systems

Nomenclature

Abbreviations:

AG	Adaptive gain
APR	Active power reserve
BESS	Battery energy storage system
CCGT	Combined-cycle gas turbine
CHP	Combined heat and power plant
DFIG	Doubly fed induction generator
FRCG	Fully rated conversion generator
HVDC	high-voltage DC
IES	Integrated energy system
MPC	Model predictive control
MPPT	Maximum power point tracking
P2H	Power to heat system
RES	Renewable energy source
RoCoF	Rate of change of frequency
SFD	Secondary frequency dip
SOPPT	Suboptimal power point tracking
VSWT	Variable speed wind turbine
WECS	Wind energy conversion system
WT	Wind turbine

Parameters and variables:

P_{wt}	Mechanical power extracted from a wind turbine
ρ	Air density
V_v	Wind speed
C_p	Power coefficient
λ	Tip speed ratio
β	Pitch angle
H_{in}	System inertia
P_{MPPT}	Maximum power
ω_{sys}	Synchronous speed
$\omega_{r,meas}$	Measured rotor speed
$\omega_{r,ref}$	Reference rotor speed
f_{meas}	Measured system frequency
f_{nom}	Nominal system frequency
ω_r	Rotor speed
k_{adap}	Adaptive gain
E_k	Kinetic energy
J	Moment of inertia
ω_{del}	De-loading rotor speed
ω_{MPPT}	Maximum rotor speed
M	Generation margin
R	Droop gain
P_{res}	Reserved wind power

1. Introduction

Electric power systems, considered as one of key subsystems belonging to large scale Integrated energy systems (IESs), have been rapidly developing over the last few decades. Integration of RESs has often been on the top of the agenda of this development [1]. Quite naturally, electrical energy has been mainly generated from primary energy sources, such as coal, oil, water, or natural gas. Nonetheless, traditional fossil fuel-fired power plants cause air pollution and carbon dioxide emission when generating electricity [2]. In order to meet the requirements of the Paris Agreement on 40% greenhouse gas emissions reduction by 2030 [3], nowadays many countries are replacing their conventional generators with RESs. For example, more than 40% electricity is expected to origin from RESs in Spain by 2020 [4]. In 2017 China installed 19.7 GW wind capacity, what is 37% of the total world installed wind capacity [5]. In 2017, Danish government already achieved 44% electricity production from wind energy [6]. In the third quarter of 2019, some 40% of the entire UK electricity generation originated from RESs, which is more than the electricity generated by the conventional plants [7]

With permanently increasing penetration of wind energy, the conventional operation, control and protection paradigms employed for a secure operation of the power system are becoming increasingly inappropriate. This is due to different dynamic characteristics introduced by RESs, such as wind turbines [8]. This is adversely impacting the performance of approaches traditionally used for the design, operation, and control of energy production, transmission and distribution. To this end, a large volume of ongoing research on aspects and prospects of transition towards 100% renewable-based energy vectors in general, and electrical energy in particular, is well justified as a timely response to these fundamental system changes [9–12].

The main motivation of the most research activities is to contribute to the approaches ensuring system frequency stability [13]. Frequency stability is the ability of power networks to maintain frequency within statutory limits and to keep balancing power generation and consumption, following a frequency event. However, increased penetration of RESs is negatively affecting system stability. For this reason, to reduce the risk of potential cascading events and catastrophic blackouts, electricity system operators define a maximum permissible level for instantaneously operating renewable generation. For instance, the permissible renewable penetration level in Ireland is 55% of the total generation [14]. Strengthening the transmission system in Ireland is thought of as a viable solution to overcoming this problem thus achieving higher decarbonisation targets [4][15].

As it is known, synchronous generators contribute to the compensation of power imbalances by releasing, or absorbing their kinetic energy following an imbalance. Since their rotor is decoupled from the grid side frequency variation, WECSs do not inherently exhibit the inertial response as that in synchronous generators. Therefore, the power system cannot expect any instantaneous extra active power contribution from WECSs. Therefore, the increased penetration of RESs and the displacement of conventional generating units is decreasing the total system inertia and APRs. This decreases the power system's ability to adequately respond to frequency events, e.g. generation outages. This is why the RoCoF is much higher in modern power systems with reduced system inertia, compared to those of conventional ones dominated by synchronous generators [16]. Therefore, in low inertia systems, the frequency nadir is more likely to fall outside of statutory limits following contingencies of the same size. In order to guarantee a more secure system operation, as well as to weaken the impacts of the integration of wind power, WTs control loops have to be adapted to the system needs. Thus, by providing the inertial control similar to what conventional generators provide during contingencies is necessary to be implemented, to ensure a stable system operation during high penetration of power electronics connected RESs [17].

Secondly, the inertia of modern power systems will not always just be reduced and may vary depending on the share of renewable generation from the whole generation mix at a specific time instant. This volatility in system inertia will introduce technical challenges when designing and setting system integrity protection schemes, e.g. under-frequency, or under-voltage load shedding. The functionality of some of these schemes may need to be carefully redefined in response to the increasing levels of RESs in the power system.
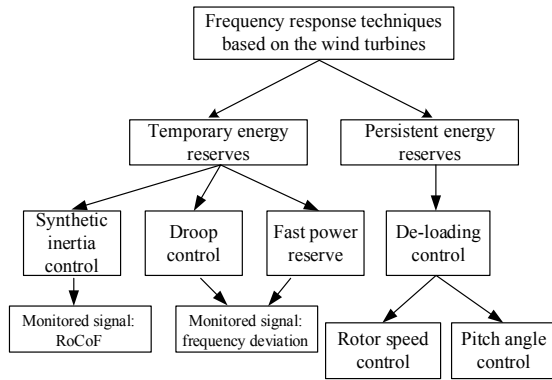
Fig. 1. Classification of frequency response techniques

So far, a number of innovative solutions have been proposed, addressing these emerging challenges related to the system inertia reduction. Recent examples include new solutions introduced within e.g. Enhanced Frequency Control Capability (EFCC) and Massive InteGRATion of power Electronic devices (MIGRATE) projects led by UK National Grid and TenneT, respectively [18,19]. Furthermore, an assessment of the technology capabilities for fast frequency response project is conducted by GE for Australian energy market operator [20]. Additionally, a new project entitled Interconnection Frequency Response proposed a set of options for maintaining reliable interconnection frequency response in USA [21]. The operational theory and power system planning of power systems with high penetration level of RESs, were parts of the national key research and development program of China [22]. EirGrid and System Operator for Northern Ireland (SONI) investigated a series of cases related to increased RoCoF [23]. All these studies indicate or prove that applying additional and adequate frequency control mechanisms is unavoidable. One of the most important requirements is that WECSs ought to provide frequency support that is normally delivered by conventional synchronously operating generating units. How a WECS should respond to a frequency event and provide optimal active power support is a complex technical question and its answer depends on the system operational characteristics. Fig. 1 summarises frequency response techniques which will be discussed in the rest of the paper.

The classification of frequency response techniques, presented in Fig. 1, is redefined in this paper, considering that the following aspects are considered: 1) different forms of energy, used for frequency control and 2) input signals, used for control approaches. Both aspects are important and worth to be investigated in several research activities in this field. On the other hand, the proposed review paper fully elaborates on the approaches dealing with the secondary frequency dips (SFD). Whereas many research works might not particularly pay enough attention to this topic, the impacts of SFD on the frequency responses would be quite obvious. This is due to the fact that the amplitude of SFD can be even larger than the first frequency nadir depending on the integration level of nonsynchronous generators [24]. With these additional controlling strategies, the WECSs are no longer decoupled from the grid. Consequently, the frequency stability of the grid can be improved/ensured.

It is to be pointed out that the discussions and reviews cannot be focused on power systems only and the frequency control in an IES is rather substantial. The hybrid concept of any energy vectors in the environment of frequency support is worthy to be noted. Also, the energy conversion system (e.g. power-to-heat system) significantly increases the integrated system's flexibility and the diversity of ancillary services. In this context, this study reviews frequency stability challenges experienced in modern power grids as a result of the integration of WECSs. Moreover, this paper reports on the available research activities to mitigate or address the influence of WECS's integration. Some control solutions, including temporary and persistent energy reserve techniques and other methodologies applied to mitigate the effects of WECSs' integration, are provided. The paper also concentrates on the involvement of WECSs to the primary frequency control and discusses the existing research gaps. The pros and cons of different controlling strategies provided by WECSs are also discussed. Moreover, the frequency control in integrated IESs is discussed for enhancing the frequency stability.

The rest of this paper is organised as follows. Section 2 elaborates on the frequency response of conventional power systems and also discusses effects of the integration of wind energy. Section 3 introduces the synthetic inertia control strategies. In Section 4, other viable frequency control techniques are explained. Section 5 illustrates the control techniques to arrest secondary frequency dips. Section 6 presents the frequency control in IESs. Future challenges and opportunities are discussed in Section 7. Finally, conclusions are drawn in Section 8.

2. Frequency responses of conventional plants versus wind Integrated energy plants

2.1. Comparison of the frequency response of conventional plant and wind-integrated plant

Conventional power plants consist of synchronously operating generators, characterised with its nominal frequency (50 or 60 Hertz). When the power system is subjected to a frequency event, e.g. loss of a generator, or a sudden connection of a large load, the system frequency can be effectively contained thanks to the inherent inertial response of synchronous generators. For a synchronous generator, the inertia constant H lies typically in the range between 4 to 7 seconds [24]. However, from the grid side viewpoint, the inertia constant of WT generators is negligible/zero, since they are electrically-decoupled from the rest of the grid. It follows that synchronous generators automatically provide support to frequency containment following a generation disturbance.

DFIGs (type 3) and FRCGs (type 4) are currently used in wind-integrated power plants. Although WECSs have a good amount of kinetic energy stored in the rotating mass of blades, this kinetic energy will not automatically participate in the frequency response due to the connection over power electronics. The reason is that WT generators are connected to the grid via AC-DC-AC power electronic converters. Differently to conventional plants, the DC voltage bus electrically decouples the rotor of WTs from the grid

frequency. Therefore, it will be a loss of opportunity if the kinetic energy of WTs is left unused while could be beneficial to grid stability otherwise. Indeed, synchronous generators speed cannot fall below 0.95 *pu* DFIGs can operate under a wide range of generator speed between 0.7 to 1.2 *pu* FRCGs can operate within an even wider range of 0.5 to 1.2 *pu* [25]. As above discussed, the progressive deployment of WECSs not only decreases the total system inertia, but also reduces the APRs in the system. Fig. 2 shows frequency response for various system inertia and APRs when the system is subjected to a generation loss of the same size. As it can be observed, the system frequency declines at a higher rate and reaches the lowest frequency nadir f_3 in the system with the smallest inertia (5 s). Fig. 2 also shows frequency response for power systems with the same inertia (10 s) and different levels of APR, system frequency decreases at a lower rate and reaches a higher frequency nadir f_1 when APR is larger. It follows that under higher penetration of RESs, frequency stability deteriorates and wear and tear of machines [26] are more likely to be experienced.
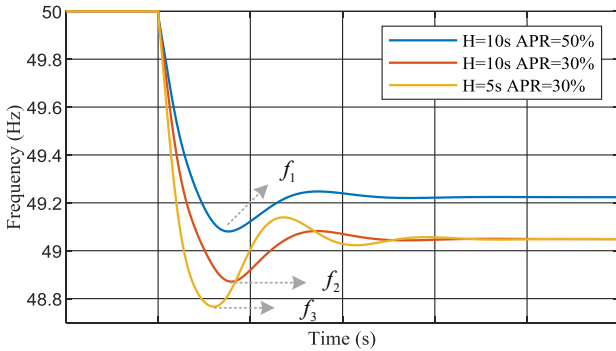
Fig. 2. System frequency response for different levels of system inertia (*H*) and APR
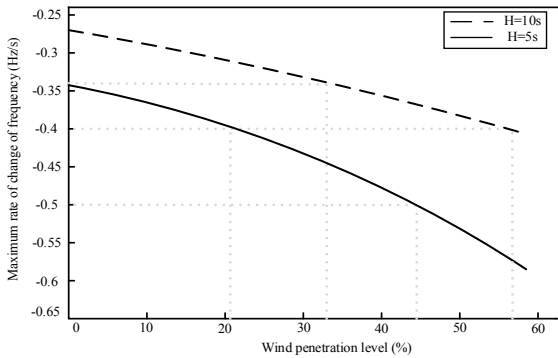
Fig. 3. Comparison of RoCoF for different system inertias [27]

In order to further explore the effects of wind power integration, Fig. 3 shows a comparison of initial RoCoFs for different wind penetration levels. Two curves represent two different systems having various inertias. As it can be concluded, following a loss of a generation with the same size, the initial RoCoF is larger in the system with the smaller inertia. Additionally, the RoCoF increases faster as the penetration level increases. This high RoCoF causes technical challenges when applying system integrity protection schemes, e.g. underfrequency load shedding [28–31], or intentional controlled system islanding [32–36].

2.2. Wind integrated energy plants

In this section, the process of converting wind energy into electrical energy delivered to the grid is described. Two widely used WECSs and the power characteristics of each are discussed.

2.2.1. Doubly fed induction generator and fully rated converter generator modelling

WECSs have been extensively studied in the open literature [37,38]. Doubly fed induction generators (DFIGs) and fully rated converter generators (FRCGs) are known as the most commonly used WECSs. A DFIG consists of a gearbox, induction generator, and AC/DC-DC/AC power converter. The stator windings are directly connected to the grid. To optimally use available wind energy, the rotor windings of DFIGs are connected to the grid via a converter, which decouples the wind generator speed from the power system frequency [39]. A very demanding regular maintenance of the slip ring, complicated assembling of brush in nacelles, and support limitation caused by crowbar circuit control are considered the main disadvantages of DFIGs.

Regarding the number and the total size of installed capacity, in modern power systems FRCGs are taking a more dominant role compared to DFIGs. The shaft of FRCGs is connected to synchronous generators with or without a gearbox and the synchronous generator is connected to the grid via a fully rated power converter. This means that the generator is entirely electrically decoupled from the main grid, thereby reducing the volume of the power system-machine interactions. However, the integration of FRCGs into the power system requires higher investment cost due to the use of a fully rated power converter. Accordingly, the cost-effective characteristic of the DFIG helps to maintain its role in the market for a foreseeable future [40]. From the technology perspective, DFIGs can maintain a unity power factor, as well as to operate at variable rotor speed with the ability to simultaneously control the amplitude and frequency of the output voltage. However, the shaft of FRCGs actually improve conversion efficiency over the full operation range of the turbines but with a higher initial investments [41].

2.2.2. Aerodynamic system

The aerodynamic system is introduced to obtain the mechanical power extracted from a WT as below:

$$P_{wt} = \frac{1}{2}\rho A V_v^3 C_p(\lambda, \beta) \qquad (1)$$

where ρ is the air density, A is the rotor swept surface, V_v is the wind speed and C_p is the power coefficient. Besides, C_p which is determined by wind and turbine speed can be expressed as [42]:

$$C_p(\lambda, \beta) = 0.5176(\frac{116}{\lambda_i} - 0.4\beta - 5)e^{-\frac{21}{\lambda_i}} + 0.0068\lambda \qquad (2)$$

$$\frac{1}{\lambda_i} = \frac{1}{\lambda + 0.08\beta} - \frac{0.035}{\beta^3 + 1} \qquad (3)$$

4

where $\lambda = \omega R / \nu$ represents the tip speed ratio. Besides, ω, R and ν are angular speed, length of the blades and wind speed, respectively. In this formula β denotes the pitch angle [43,44]. According to Betz limit [45], the maximum value of C_{p_max} is 0.593. It follows that the maximum machinal power the WT can deliver to the grid is [42]

$$P_{wt\_max} = \frac{\rho \pi R^5 C_{p\_max}}{2\lambda_{opt}^3} \omega_{opt}^3 \qquad (4)$$

2.2.3. Maximum power point tracking

In this section, the *MPPT technique*, based on the wind speed estimation, is introduced [46,47]. This technique is used for determining the maximum power that can be delivered from WTs for different wind speeds. The MPPT curve shown in Fig. 4, i.e., the blue curve, can be divided into four operation sections. The first section (M-N) corresponds to conditions in which the active power contributed from the WT follows a linear trend. Then, the WT starts operating at its MPPT mode (N-P) and contributing maximum power to the grid. In the third section (P-Q), the WT operates at a constant rotor speed regime, in order to avoid the rotor overspeed. It is worth noting that the wind power available at high speeds may exceed the power indicated by the MPPT curve. If wind speed exceeds the rated value (Q), to guarantee a rated output power the constant power mode is switched on.
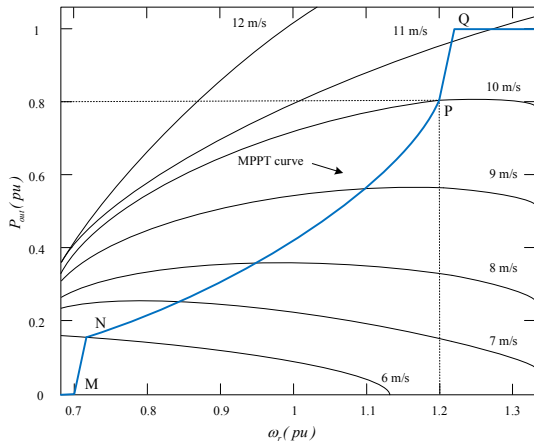
Fig. 4. Active power-rotor speed curve of a DFIG for different wind speeds [44]

Considering the intermittence of captured wind power [48], the reduction of turbine mechanical stress [49], interactions between conventional and renewable power plants [50] and wind direction conditions [51], a more precise MPPT models can be deployed for improving the wind energy production.

3. Synthetic inertia control

It is a well-established fact that the kinetic energy stored in the rotating blades of WTs will not automatically participate in frequency control of the power system. Nevertheless, VSWTs can easily emulate a similar inertial response to that of synchronous generators by implementing appropriate control mechanisms [52]. This is to maintain system frequency within a permissible range upon generation losses

resulting in an active power imbalance in the power system. This can be accomplished by monitoring RoCoF and properly adjusting the active power delivered to the grid.

In [53], the term *synthetic inertia* is defined as a process of controlling the active power of a unit such that it is proportional to the RoCoF at the terminal of that unit. One-loop inertial response and two-loop inertial response are two commonly used options. The extra active power delivered by the one-loop control is proportional only to the measured RoCoF [53–57]. Detecting both the RoCoF and the frequency deviations is required in the two-loop control approach [58,59]. Block diagram of the one-loop control alternative is depicted in Fig. 5. The synthetic inertia active power P_{in} contributed from the additional control loop is shown in the upper dashed block. Being proportional to the RoCoF and synthetic inertia constant H_{in}, this power is calculated as follows:

$$P_{in} = 2H_{in} \times \frac{d\omega_{sys}}{dt} \times \omega_{sys} \qquad (5)$$

The lower block represents how the active power is delivered by the WT. Denoted by P_{MPPT}, this power is determined by a PI controller that compares the measured rotor speed, $\omega_{r,meas}$, with a reference rotor speed, $\omega_{r,ref}$.
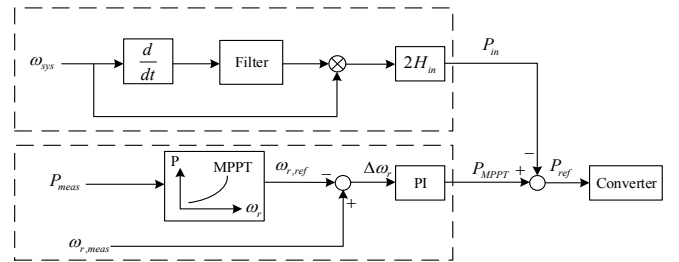
Fig. 5. Synthetic inertia one-loop control design [60]

In [61], the authors propose an advanced two-loop synthetic inertia control approach. In this design, the extra active power, P_{extra}, is determined by two loops, i.e., the RoCoF loop and the *droop loop*, as shown in Fig. 6. As demonstrated in the upper block from this figure, the RoCoF and the frequency deviation Δf are obtained by directly measuring the grid frequency. Here it is essential to have an accurate approach for measurement of frequency and its rate of change. Among a number of numerical algorithms for their measurement, those based on parameter estimation demonstrated a high level of robustness and accuracy [62–66]. The synthetic inertia is proportional to the inertia constant K_{in} as below:

$$P_{in} = -K_{in} \frac{df}{dt} \qquad (6)$$

The second control loop adds an additional power, P_d, which is calculated as follows:

$$P_d = -\frac{1}{R}\Delta f = -K_d \Delta f \qquad (7)$$

In this respect, an activation scheme is proposed in [61] that uses an 'over/under frequency trigger' and the 'maximum frequency gradient trigger' to provide a more effective frequency control following a frequency event.

These are a number of advantages when applying one- or two-loop synthetic inertia controls. Both of them enable WT to participate in the frequency control process, thereby reducing the system RoCoF and delaying/removing a need for underfrequency load shedding in the system. Nonetheless, the two-loop control provides an additional power that is proportional to the frequency deviation, Δf, which more precisely emulates synchronous generators' behaviour under equivalent conditions and guarantees to bring the grid frequency back to nominal frequency as quicker as possible.
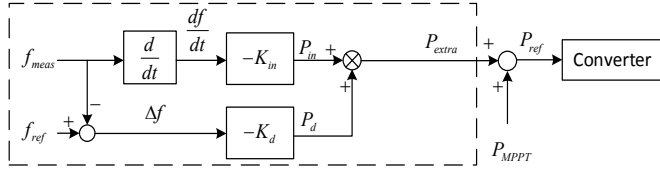
Fig. 6. Synthetic inertia two-loop control design [61]

4. Primary frequency response

Various frequency controls, depending on different forms of the power reserve, have been proposed so for. The core purpose of all these controls is to overcome frequency instability problems introduced by wind power integration. Indeed, these control mechanisms enable WECSs to effectively contribute to the frequency support in the system, as will be discussed in detail in this section.

4.1. Temporary energy reserves

Mandated by the latest grid code (see *COMMISSION REGULATION (EU) 2016/631*), the WECSs are expected to possess the ability to participate in frequency control upon a need, in order to limit the RoCoFs [67]. Temporary energy reserves can be realised by resorting to the kinetic energy stored in the rotor of WTs. Relating to temporary energy reserves, over the recent years three control approaches have been introduced. These approaches are a) droop control and b) fast power reserve. The droop control releases some extra power in proportion to the frequency deviation measured. The fast power reserve approach focuses on the fast kinetic energy release in a stepwise incremental manner.

4.1.1. Droop control

The aim of the droop control is to mimic similar frequency droop characteristics to that of the governor of a conventional synchronous generator and to contribute to both transient and steady-state frequency control. References [68–74] discuss the performance of frequency support enabled by the droop control. The slope of the power-frequency droop characteristic affects the frequency nadir and frequency recovery after a loss of generation disturbance [72][75]. The droop control alters the WT output and provides frequency support based on the grid frequency deviation, Δf. The following equation refers to this behaviour:

$$\Delta P = P_1 - P_0 = -\frac{f_{meas} - f_{nom}}{R} = -\frac{\Delta f}{R} \tag{8}$$

where $\frac{1}{R}$ is the droop coefficient, P_0 and f_{nom} are initial WT power and frequency, respectively. Besides, P_1 and f_{meas} are the adjusted WT power and frequency, respectively. Resulting from this control, the WT output power increases from P_0 to P_1 as the system frequency decreases from f_{nom} to f_{meas}. However, the main drawback of this droop scheme is frequency inadaptability due to the fixed gain chosen in the control loop. In other words, if a large gain is used to improve the frequency nadir, it may cause unnecessary over-deceleration of the rotor speed.

An improved droop scheme is proposed in [76], aimed at overcoming the insensitivity of the droop loop to the initial frequency deviation, the droop gain is tuned dynamically based on the measured RoCoF. The relationship between the droop gain and the RoCoF is defined for a fixed rotor speed prior to the disturbance. Nonetheless, this still might cause over-deceleration if an additional disturbance occurs. To resolve this problem, a slightly modified scheme is proposed in [77] in which the adaptive gain is determined with respect to both RoCoF and rotor speed. The extra active power, P_{extra}, can be expressed as:

$$P_{extra} = k_{adap}(\frac{df}{dt}, \omega_r) \cdot \Delta f \tag{9}$$

where $k_{adap}(\frac{df}{dt}, \omega_r)$ represents the adaptive gain and Δf represents the frequency deviation. The adaptive gain is altered with the RoCoF and rotor speed, which is shown in Fig. 7. Also the adaptive gain takes the maximum value if the RoCoF is less than -0.05 Hz/s and the rotor speed is at its maximum operating speeding speed. Then k_{adap} decreases with both RoCoF and rotor speed, until the frequency reaches frequency nadir. This is to prevent the system from suffering a SFD when rotor speed decelerates to the minimum operating limit (0.7 pu). After reaching the frequency nadir, parameter k_{adap} only decreases with rotor speed to guarantee that no excessive kinetic energy will be released. The main advantage of this control scheme is that it maintains the kinetic energy available for a subsequent disturbance.
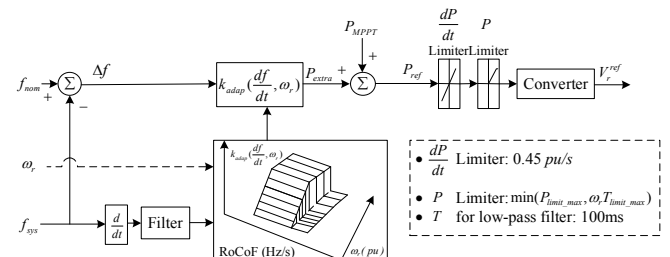
Fig. 7. Adaptive short-term frequency support control scheme associated with the concept of an adaptive gain [77]

Reference [72] puts forward a novel time-variable droop scheme. To ensure the pre-disturbance active power reference $P_{ref,pre}$ matches the active power reference generated during the frequency support period, $P_{ref,fs}$, a negative droop is added to the frequency support loop, as below:

$$\Delta E_k = \int_{t_{rec}} D^{'}(t)\Delta f(t)dt \qquad (10)$$

In Equation (10), ΔE_k is the change of kinetic energy of the WT, $D^{'}(t)$ is the negative droop function and t_{rec} is the recovery time which makes $P_{ref,pre}$ equal to $P_{ref,fs}$. The time-variable droop characteristic follows a function of $\frac{g(t)}{R}$, where $g(t)$ is a properly defined time-variable function. As shown in Fig. 8, the droop coefficient remains constant in the first one third of the frequency support period t_{sup}, because a maximum wind power is needed for arresting the frequency decline immediately after the disturbance. In the rest of t_{sup}, $g(t)$ gradually is reduced to zero where $P_{ref,pre}$ is still smaller than $P_{ref,fs}$. After system frequency reaches the frequency nadir, $g(t)$ continuously decreases to a negative value until $P_{ref,pre}$ matches $P_{ref,fs}$. This gradual change of the droop parameter will ensure a smooth exchange of energy between the grid and WECSs in addition to removing the ripples in frequency that otherwise results from cascaded switching caused by the control systems of the WECS.
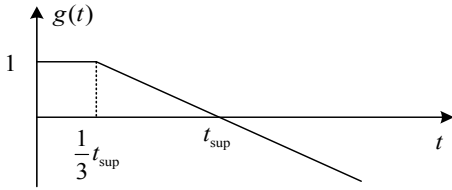
Fig. 8. Frequency support control with time-variable droop characteristic proposed in [72]

4.1.2. Fast power reserve control

Fast power reserve control is also known as rotor kinetic energy control [78,79]. In the case of a sudden frequency event, the abnormal frequency behaviour can be detected and recovered by temporarily releasing a stepwise kinetic energy within a short time window. In [71], delivering some 10% more active power than the nominal active power within 10 seconds is defined as the fast power reserve control, which is implemented to support the frequency following a generation disturbance. The kinetic energy E_k extracted from the WT can be expressed as:

$$E_k = \frac{1}{2}J\omega^2 \qquad (11)$$

where J and ω are the moment of inertia of the WT and rotor rotational speed, respectively. When a loss of generation disturbance occurs in the power system,

$$\Delta E = P_{const}t = \frac{1}{2}J(\omega_2^2 - \omega_1^2) \qquad (12)$$

where P_{const} is the constant active power provided by the WT. Besides, t is the fast power delivering time since the disturbance inception, ω_1 represents the rotor rotational speed before the disturbance and ω_2 represents the rotor

rotational speed at time t. Therefore, the reference rotor speed is defined as:

$$\omega_{r,ref} = \omega_1 = \sqrt{\omega_2^2 - 2\frac{P_{const}t}{J}} \qquad (13)$$

as shown in Fig. 9. Then the change of rotor rotational speed $\Delta\omega_r$ can be obtained and sent to a PI controller that is used to change the reference active power point P_{ref}.
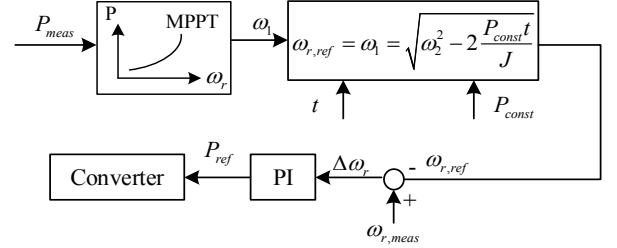
Fig. 9. Fast power reserve control loop [71]

A similar approach called *temporary over-production approach* is presented in [80], addressing the capability of VSWTs for injecting temporary power overproduction. The dashed curve and solid curve shown in Fig. 10 are WT (static) production power and blade's mechanical power in constant wind speed condition, respectively. The input signal, i.e., the system frequency f, is used to monitor the frequency dip, thus adding active power overproduction ΔP_{OP} to arrest the frequency decline.
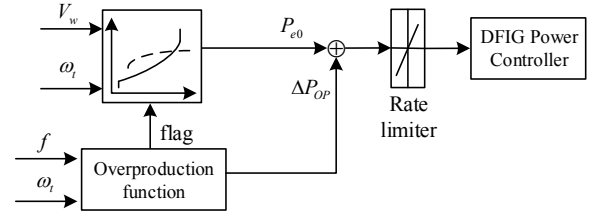
Fig. 10. Temporary over-production control [80]

Fig. 11 (a) illustrates how the active power changes with the rotor speed, following a sudden frequency event, after implementing the over-production scheme. Frequency support starts at the point A. A constant temporary over-produced power ΔP_{OP} is added to the initial reference power point P_{e0} to increase the WT output power to $P_{e0}^{'}$ (between B and C). Once frequency support is no longer required or rotor decelerates to its minimum value 0.7 pu, the rotor speed starts to recover to its pre-disturbance value from D to E. This results from the application of the accelerating power P_{acc}, which subsequently changes the reference power point to $P_m - P_{acc}$. Indeed, the determination of P_{acc} following the mechanical power trajectory (the blue line) rather than maximum power point tracking trajectory (the green line) can avoid a SFD due to the smaller active power reduction. Nevertheless, the recovery time of rotor speed can be prolonged by applying P_{acc}. Therefore, an optimal trade-off between the recovery time of rotor speed and the amplitude of SFD is deemed necessary.
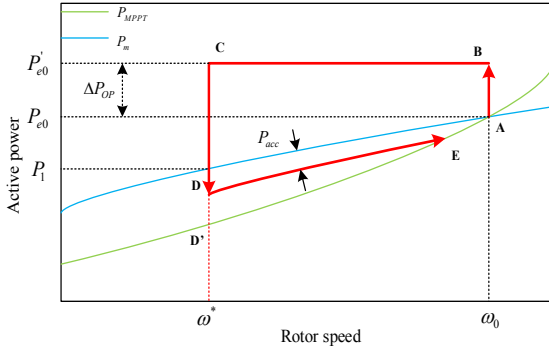
(a) Power-rotor speed trajectory
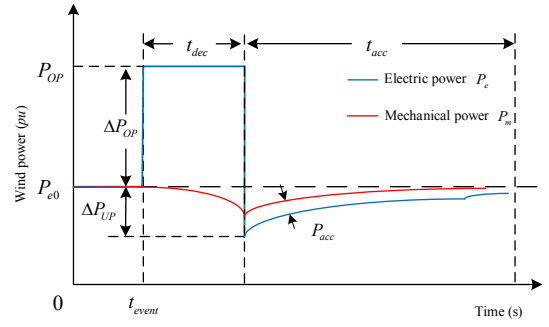
(b) Wind output power in the time domain

Fig. 11. Characteristics of the temporary over-production scheme [80]

Table 1 Summary of temporary energy reserves

Approaches	Control	Contributions	Concerns
[53–57]	Adding synthetic inertia power based on RoCoF and frequency deviation.	Declining the RoCoF at the beginning of the frequency disturbances.	1. Requiring de-loading control or adding extra energy storage system. 2. It will cause SFD after the frequency support.
[77]	Adding extra power based on an adaptively-changed droop loop.	An adaptive droop gain developed based on RoCoF and rotor speed of WTs, which avoids the over-deceleration.	The assumption of constant wind speed is not realistic.
[72]	Contributing frequency support based on time-variable droop gain.	Preventing large frequency excursions, SFD and facilitating recovery of the kinetic energy of WTs.	Test system is rather simple.
[80]	Providing extra active power output on top of available production of WTs.	Utilising the flexibility of WTs under various wind speeds.	1. Trade-off between recovery time of rotor speed and amplitude of SFD. 2. Lack of consideration of interaction of WTs in wind farms.
[81]	Providing extra power proportional to the available kinetic energy.	Considering the power efficiency of singe WT in wind farms.	Stability performance has not been proved analytically.

In order to accurately determine the wind power, the impacts brought by the wake effect is considered. Wind speed prediction in ultra-short periods is addressed in [82–84]. Therefore, the active power forecasted by a high fidelity mathematical models, or deep learning neural networks, can significantly improve the accuracy of the wind energy approximation. These research works not only provide layout guidelines for wind farms, but also deliver a more precise wind energy estimation to the system operators. In this context, the wake effect refers to the fact that the wind speed arriving at a downstream WT generator drops after travelling through an upstream WT generator. Indeed, different WT generators operate at different MPPT points in a wind farm. Wake effect has been widely explored in [85–93], discussing the effects of decaying wind speed from technical and economic perspectives. Reference [87] assumes wake wind speed is linearly expanded within wind power plants due to wind directions and overlapping shadows.

To account for wake effect, a fixed gain cannot be applied to wind power plants because each WT operates at different speed and delivers different output power. As shown in Fig. 12, only the frequency deviation ΔP_i is used in the additional control loop because the RoCoF calculation may result in potential errors due to inaccurate measured frequency. The adaptive gain $AG_i(\omega_i)$ is proportional to the available kinetic energy of the WT, i.e., ΔE_i. This kinetic energy can be expressed as follows

$$AG_i(\omega_i) \propto \Delta E_i = H(\omega_i^2 - \omega_{min}^2) \qquad (14)$$

where H is the inertia constant. Besides, ω_i and ω_{min} are instant rotor speed and regulated minimum rotor speed, respectively. Thus, at the beginning of a disturbance, a certain amount of kinetic energy can be released depending on the stored kinetic energy in the WT. WTs that have a greater amount of the available kinetic energy are set to have a larger gain and vice versa:

$$AG_i(\omega_i) = C(\omega_i^2 - \omega_{min}^2),$$
$$\text{when } \omega_i < \omega_{max} \qquad (15)$$

$$AG_i(\omega_i) = C(\omega_{max}^2 - \omega_{min}^2),$$
$$\text{when } \omega_i \geq \omega_{max} \qquad (16)$$

In order to avoid over-deceleration, the adaptive gain is reduced once the ω_i is decreased. A large value of C may still result in a massive power decrease after reaching the frequency nadir, which subsequently may result in a SFD. Simulation results show that both improving frequency nadir and preventing over-deceleration can be achieved by implementing the proposed scheme.
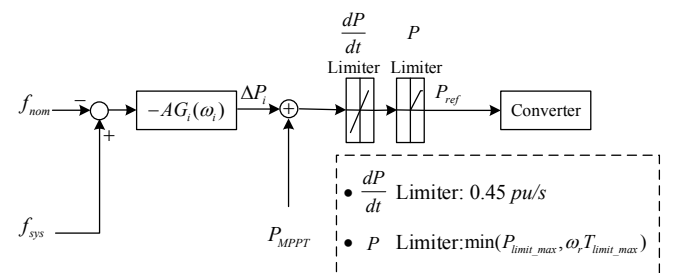
Fig. 12. Stable inertial control scheme using adaptive gains $-AG_i(\omega_i)$ [81]

Table 1 summaries and compares majority of the temporary energy reserves discussed in this paper.

4.2. Persistent energy reserves

Regarding the optimal operation of VSWTs and the use of the available wind energy, they should deliver a maximum active power to the grid with respect to the wind speed. This can be easily achieved by operating along the MPPT curve shown in Fig. 4. By doing so, however, the WECS will not be capable of providing prolonged frequency support. To resolve this issue, a certain amount of maximum possible power should be left unextracted by the WT unless there is a justified operational necessity. This is normally referred to as *de-loading control*, enabling WTs to act as a persistent energy reserve. In this context, two commonly used control schemes are explained here, namely the *rotor speed control* and the *pitch angle control*.

4.2.1. Rotor speed control

A DFIG usually deliver maximum power, determined by the MPPT curve (the blue line shown in Fig. 13). To provide a persistent frequency support, a de-loading operation is required. This can be achieved by properly shifting the WT operating point to the left or right side of the MPPT curve. Moving from the MPPT curve to the 10% de-loaded curve (red curve) on the left side of MPPT reduces the rotor speed. On contrary, the green line can be obtained by increasing the rotor speed, which is called *over-speed control*. The 10% de-loaded curve on the right-hand side of the MPPT curve is normally the preferred option. This is to avoid interference stability problems caused by the deceleration control [52].
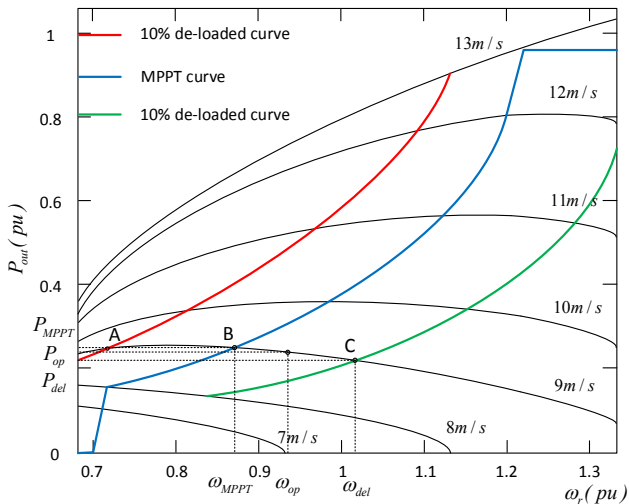
Fig. 13. Power-rotor speed curves for a WT deloaded by 10%[56][79]

For implementing the over-speed control, the operating point, P_{op}, lying between the points B and C, is obtained according to [94][52]:

$$P_{op} = P_{del} + (P_{MPPT} - P_{del}) \times (\frac{\omega_{del} - \omega_{op}}{\omega_{del} - \omega_{MPPT}}) \qquad (17)$$

where P_{del} and P_{MPPT} are de-loading power and maximum power, respectively. The former is the WT power corresponding to the interception point of the green line and the mechanical power curve. Here ω_{del}, ω_{op} and ω_{MPPT} are denote de-loading rotor speed, operating rotor speed and maximum rotor speed, respectively. With respect to the convertor size, the rotor speed is allowed to vary within a predetermined range, e.g., 0.7 *pu* and 1.2 *pu* The selection of the speed range is carried out based on the economic optimisation of the investment costs and increased efficiency [95]. Therefore, during high wind speed conditions, the over-speeding control is not suitable due to the rotor speed limits.

4.2.2. Pitch angle control

An accurate and complete pitch angle model is crucial for applying de-loading control [96,97]. In [97], a novel blade pitch model with an optimal pitch control has been designed, manufactured and verified using wind tunnel tests. Regarding de-loading operation, pitch angle control de-loads the WT operating point from MPPT curve by increasing the blade's pitch angle. In [98,99], C_p is reduced based on the Equation (2) which decreases the output wind power. This control is essentially activated when a WT reaches its rated speed, whereas the speed controller has been disabled or has failed to respond [100,101]. Fig. 14 shows the power-rotor speed curves of a typical 1.5 MW wind turbine for different values of pitch angle under constant wind speed. The pitch angle controller de-loads a WT at the point A at which the rotational speed of the WT reaches its rated speed. Then the operating point of the WT is shifted from A to B. This "increased pitch angle" de-loads the wind power by 10%, while the rotational speed remains constant.
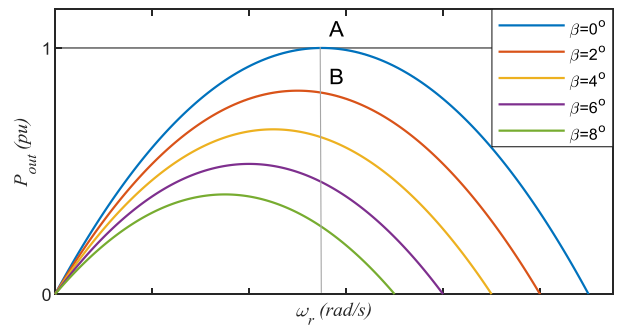
Fig. 14. 1.5 MW WECS power-rotor speed curves [102]

A coordinated frequency support control is proposed in [94], by integrating the de-loading control and a variable droop control with a properly selected droop gain. The gain is determined based on the approach presented in [103] using a small-signal approach.

9
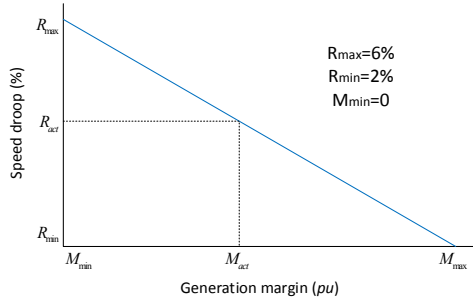
Fig. 15. Droop variation for different generation margins [94]

Droop gains are adjusted with respect to the reserved power of the corresponding WT. The dynamic variation of the droop gain is obtained by linearly decreasing the droop value for larger power reserve margins as shown in Fig. 15. In order to have a maximum margin of the WT, M_{max}, a minimum droop gain R_{min} is needed. The droop gain R_{act} is given by:

$$R_{act} = R_{max} - (R_{max} - R_{min}) \times (\frac{M_{act} - M_{min}}{M_{max} - M_{min}}) \qquad (18)$$

where M_{min} and R_{max} are the minimum margin of the WT and its maximum droop gain, respectively. M_{act} is the actual generation margin of the WT. The power margin, P_{margin}, can be expressed as follows:

$$P_{margin} = P_{max} - P_{out} \qquad (19)$$

where P_{max} is the MPPT power point and P_{out} is the wind power output. In this respect, P_{margin} changes from M_{min} to M_{max}. The WT operates following the MPPT curve at M_{min}, whereas M_{max} depends on the de-loading curve. Based on the de-loading control, the variable droop control ensures that WT delivers the maximum output power and operates in a stable condition under low wind speed regimes.

In [69], a SOPPT control is proposed, based on the delta control approach proposed in [104] and the rotor speed-based de-loading control approach. The delta control reserves a constant power or a constant percentage of the available power for emergency conditions.

The SOPPT control is taking advantage of the two schemes for delta control at various wind speeds. In Fig. 16, the orange (dotted) line and the green line represent the SOPPT with 20% power reserve curve and the SOPPT with $0.05\,pu$ power reserve curve, respectively. To overcome disadvantages of the delta control, the authors define the point Y', i.e., where the orange and green lines intercept, as the wind speed boundary (which is set to 7.7 m/s). In addition, the same amount of power can be reserved by these two schemes. When wind speed is smaller than 7.7 m/s, the proposed SOPPT curve follows the green line. However, when the wind speed is above the boundary, the proposed SOPPT curve switches to the orange line until point Z' at which the constant rotor speed mode is triggered.
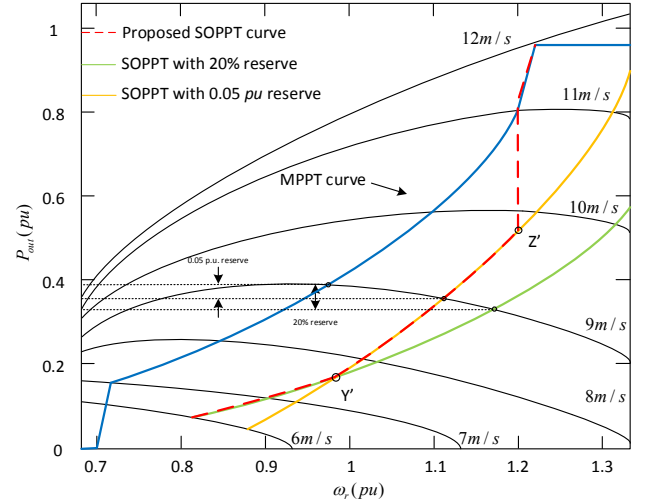
Fig. 16. SOPPT strategy – Power-speed characteristic [69]

The amount of the reserve power, P_{res}, can be obtained from Equation (1), as below:

$$P_{rev} = \frac{1}{2} \rho A V_v^3 [C_p(\lambda_1, \beta_1) - C_p(\lambda_2, \beta_2)] \qquad (20)$$

where $C_p(\lambda_1, \beta_1)$ and $C_p(\lambda_2, \beta_2)$ are the power efficiency under MPPT and SOPPT curves, respectively. Since $C_p(\lambda_1, \beta_1)$ can be obtained by checking MPPT curve, λ_2 and β_2 are subsequently changed to maintain the required P_{rev}.

Reference [79] elaborates on determining the applicable range of the two above described de-loading methods. Firstly, the limited over-speed de-loading curve is proposed based on the de-loading level, and the de-loading level is determined with respect to both the rotor and wind speed. A more advanced coordinated active power control is proposed in [105], which precisely defines the coordinated operating zone of the rotor speed and pitch angle control. Nevertheless, robust control of the rotor speed due to the unpredictive wind speed might be challenging in both approaches. This can result in a frequent switching operation between the pitch angle and rotor speed control, which exacerbates the wear of mechanical parts.

In order to make the most use of releasable kinetic energy of WTs and to increase the revenue of wind farms, the droop control is applied to de-loaded WTs [106,107]. In [94], the approach takes the maximum limit of the de-loaded WT rotor speed into consideration, to prevent the potential instability due to low rotor speed. However, this approach requires communication between WT generators in a wind farm.

In [108] a droop coefficient is proposed, based on the reserved energy of WTs for primary frequency response. It also discusses the coordination between WTs and synchronous generators. However, both approaches mentioned require the performance of WTs, which depends on wind speed measurements. To mitigate the inaccuracy of the wind speed measurements, a so-called *efficiency droop control approach* is introduced in [109]. In this approach, the de-loaded wind power is related to the tip ratio rather than the wind speed, as discussed in the previous section. In [106], techniques based on torque-droop and power-droop are proposed. Their performances are evaluated in terms of both the transient and steady-state responses. It should be noted

10

that a higher rate of change of power due to the implementation of these techniques increases the mechanical tension of the WT, leading to a higher maintenance cost. In order to determine the amount of kinetic energy provided by each control scheme, a coordination of the droop and de-loading controls is necessary.

In order to reduce the mechanical stress of WECSs, in [110] a *torque limit-based control* technique is proposed. This technique makes the released kinetic energy more flexible by linearizing the initially non-linear relationship between rotor speed and its operating point.

5. Control techniques to arrest secondary frequency dips

In previous sections, frequency control techniques emulating the system inertia and contributing to the frequency support are discussed. However, releasing the kinetic energy stored in the rotor causes rotor deceleration. This means that the frequency support from VSWTs has to be terminated when the rotor speed reaches its minimum value. This minimum value has to do with the stable operation of the VSWT. This termination results in a SFD because of the sudden loss of the active power provided by the WT [111–116]. In many cases, the SFD may be even larger than the first frequency nadir caused by the frequency event. The higher the penetration level of the wind energy, the larger the SFD [111]. According to [114], after losing the extra power contribution from WTs, a *gradual power transition* can be an effective approach to avoid the SFD. By comparing Fig. 17 with Fig. 11 (b), the authors in [44] demonstrate the importance of carefully controlling the frequency behaviour during the supporting period. The transition between overproduction and underproduction should follow a cautiously determined slope to avoid over-deceleration and to mitigate a SFD caused by the sudden drop of the active power.
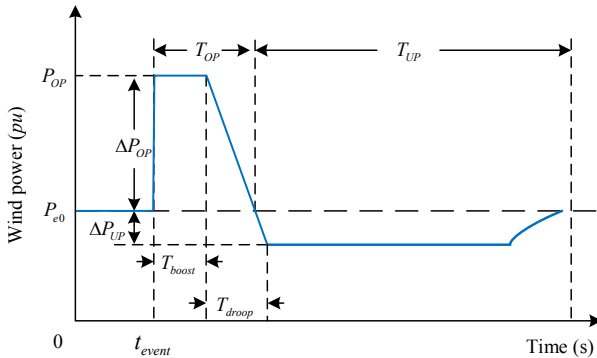
Fig. 17. Proposed shape for short-term extra active power [44]

A stable adaptive inertial control scheme is proposed in [116], aimed at improving the frequency nadir and RoCoF. Here, a minimal possible SFD is also a target during the wind power reduction. During the rotor deceleration period, t_{dec}, a proposed reference power point, P_{ref}', following the power tracking point trajectory (shown in purple colour in Fig. 18 (a)) is set to a value which is larger than P_{MPPT} (from B to C shown in Fig. 18 (a)) by ΔP_{OP}. Therefore, the approach of releasing more power can improve the frequency nadir and

RoCoF. The frequency support continues until the point C in Fig. 18 (a). Afterwards, the rotor speed starts recovering. During the rotor acceleration period, t_{acc}, the reference power point, P_{ref}'', is switched to a value inside the rotor speed range of ω^* and ω_{MPPT} as below:

$$P_{ref}'' = P^* - 0.03\,pu \qquad (21)$$

where P^* is the active power at which the frequency support is accomplished. Then, P_{ref}'' is maintained until the active power output reaches the point E. Afterwards, the reference power point returns to P_{MPPT}. Comparing with the scheme proposed in [44], the smaller power reduction results in a smaller SFD. The main challenge here is the fact that the wind speed is difficult to be predicted during the power transition. In this context, a coordination between the available WT active power reserve from one hand and the HVDC interconnectors' active power control/capabilities from another hand, has to be considered, as tackled in [117]. The proposed approach compensates the SFD by changing the dispatches of frequency response reserve in various independent nonsynchronous power grids.
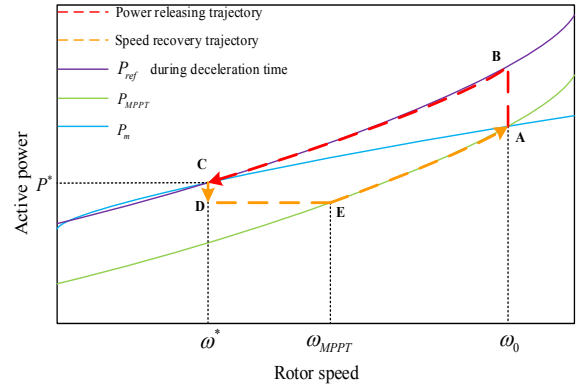
(a) Power-rotor speed
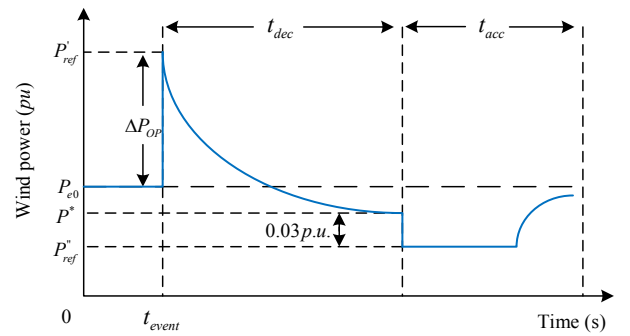
(b) Wind output power in the time domain
Fig. 18. Stable adaptive inertial control scheme [116]

To minimize the size of the SFD, which can be dangerous from the perspective of system frequency stability, a novel scheme is proposed in [118] and its application strategy is proposed in [119]. Comparing the conventional fast power reserve approaches, this scheme focuses on the correlation between the size of the SFD and the termination time of the frequency support from WTs. In [118], the optimal time for terminating the frequency support from WTs is analytically derived as fixed termination time to minimize the size of the

SFD, but the parameters of the system frequency response model must be known. In [119], these parameters are estimated and the incremental active power of the fast power reserve approach is also determined. As such, the fixed termination time is suitable for practical application.

6. Frequency control in integrated energy systems

IESs, also named as multi-energy systems, provide different forms of energy, e.g. heating/cooling, electricity, or gas to the end users. An IES can improve the flexibility, stability, and efficiency of the whole energy system. For the sake of frequency control scheme in IESs, a coordinated and hierarchical approach should be deployed. It is notable that the high-cost reserves and communication burden among RESs are inevitable. On the other hand, the combined sources in an IES can be arbitrary, which increases the complexity of investigating the capability of frequency control schemes. In this context, the energy conversion strategies and new supervisory controlling frameworks are proposed.

When WECSs are integrated into a combined cycle gas turbine (CCGT) based power systems, frequency events could bring threatening dynamic interactions. This is because active power output is not entirely determined by the governor response during the frequency deviations of the power network [121]. . Additionally, [121,122] illustrate the load frequency management approach in conventional CCGT and the impact of the phase lock loop on system dynamics. On top of that, the combined effect of electric vehicles and DC links for load frequency management schemes in a three-area system is elaborated in [123]. The impacts on transmission interconnection is investigated in [124]. HVDC link plays a crucial-linking role in facilitating the frequency restoration due to WECSs, remotely connected to load centres in most cases. In [42], HVDC link is responsible for WECSs to observe the change of grid frequency based on only local measurements. Based on this characteristic of the HVDC link, a coordinated control dealing with subsequential frequency dips is developed for effectively using the conversed energy. Similar schemes are discussed in [125] and [126]. However, the main disadvantage of the schemes is in the requirement of a large volume of capacitors. In [127], an optimization model for a regional electricity grid, is depicted in the consideration of the cost-minimal generation, transmission, and storage capacities required to maintain the frequency stability.

In order to increase the penetration level of RESs, the integration of power to heat systems (P2Hs) is aimed to absorb the excessive electricity from the grid. On the other hand, when integrated to CHP, the P2H system is functional as heat storage systems, and preferably connected to district heating systems. In [128], a primary frequency control contributed by hybrid battery energy storage system (BESS) and P2H system is presented. BESS responds firstly to the change of the grid frequency instead of synchronous generators doing so. The obtained results prove the feasibility, and this combined control scheme can dramatically reduce the battery investment compared to the stand-alone BESS. However, simulation results are only carried out based on the medium level charged BESS. Further research should be focused on a higher charge level with consideration of battery decaying. In [129] a multi-criteria operation strategy in virtual power plant is presented. It is based on the heat demand and generation prediction, which helps enhancing the integrated systems' flexibility.

In order to overcome the slow responding speed of combined heat and power (CHP), a coordinated control scheme for CHP generation with an embedded battery is proposed in [130]. The responsibility of BESS is to quickly compensate the imbalance between the output of the CHP and the required power. In addition, the power outputs of CHP and battery are determined by the heat demand, frequency response demand and battery state restoration requirement. This control strategy enhances the flexibility of CHP; however, the future work should pay attention on optimal determination of BESS size for contributing the frequency support.

Both [131] and [132] consider the interaction between different power system frequency related service providers, in order to preserves the power system frequency stability. The adequate models of BESS, photovoltaic system, wind turbines and CHP are developed in [131]. A distributed optimal frequency control approach is proposed in [132]. The approach considers constraints and flexibility from district heat system, but also limitations posed from transmission grid and demand side. In addition, this approach is based on limited input data, i.e. measurements, as well as low data transfer requirements, reducing by this communication burden existing in the traditional centralised frequency control schemes.

On the other hand, the frequency control constraints in IESs draw researchers' attention to the hierarchical system frequency managements and controls [133,134]. In general, a framework for hierarchical frequency control predominantly depends on the energy resources connected to the systems. Application of the supervisory model predictive control (MPC) derived from artificial neural network approach for hierarchical two-level IESs is proposed in [135], [136]. Similarly, a two-level hierarchical control applying on both transmission and distribution energy systems are proposed in [137,138], where a fast frequency control mechanism is presented. A combination of *centralized plus distributed approach* is adopted for the coordinated control strategy presented in [139]. It is organized into three levels, as follows: a) IES-level, b) micro-energy internet-level and c) component-level. Furthermore, the communication design for each level's control is optimized.

7. Discussions on challenges

As previously pointed out, by integrating a large number of RESs into the power system, a number of technical challenges can appear. This section elaborates on current and future challenges which have to be considered to ensure optimal integration of RESs and simultaneously equally secure and reliable operation of the existing bulk power system.

7.1. Discussions on current challenges

The aim of the usage of the temporary energy reserve for system frequency control is to cope with frequency events leading to large active power imbalances. Under these circumstances is necessary to reduce the system frequency decline, the RoCoF, as well as to improve the frequency nadir. As previously discussed, this is achieved by managing the available kinetic energy of the WT rotor. However, a

temporary frequency support is followed by a SFD, which might be even deeper and more dangerous than the primary frequency dip. On the other hand, the provision of the persistent energy reserves requires WTs to operate in a suboptimal mode to be able to provide a long-term frequency support upon need. This would inevitably result in a decrease in annual revenues of wind farms. Therefore, a coordination between two types of energy reserves is a topic requiring much attention in future. This is to ensure system frequency stability without reducing wind farm profitability.

By now, research has been predominantly focused on enhancing the WT performance, but individually. From the bulk power system point of view, however, the overall contribution of kinetic energy by wind farms would be of major importance [140,141]. For a wind farm, wind energy mainly varies with wake effect [142] and wind farm layout [143]. As a result, each WT operates at various operating state. This means that the available kinetic energy, which can be extracted from each WT, would be different. Based on these considerations, the wind farm-based kinetic energy control schemes ought to be facilitated by evaluating each individual WT operation.

Furthermore, the challenges and difficulties resulting from the implementation of HVDC transmission links, i.e. interconnectors, in RESs dominated systems are becoming increasingly important. Traditional generation and other electromagnetic energy conversion devices can tolerate overvoltage and overcurrent problems within several cycles of fundamental frequency. However, HVDC links based on power electronics could be permanently damaged within only microseconds as a result of faults. Therefore, convertors utilised in HVDC transmission links have to be carefully designed to improve their overloading capability [144]. Another major problem are harmonics and high-frequency resonances caused by fast control, switching operation and dynamics of power electronics in large wind farms [145,146]. These may result in low power quality or frequent tripping of WTs, which would damage sensitive devices. Growing harmonic oscillations may also result in malfunction or misoperation of the protection system, and should not be neglected [19][147].

Last but not least, conditions in which generated active power is larger than the consumed one, is equally important challenge and has to be properly addressed in systems with a high penetration of RESs. Such situations are quite common in economically underdeveloped regions in which renewable energy is dominating. One of the main reasons of having this issue is lack of enough transmission capacity for transferring surplus power to regions where this power is needed. Researchers in [148–151] have shown that the optimal sizing the storage systems can help to reduce potential waste of wind energy in remote areas.

A new generation of smart control technology and interactive business model called *virtual power plant* (VPP) [152,153] initiated by the State Grid Corporation of China has attracted interest of all parties. A VPP integrates all types of distributed generators, storage systems, controllable loads and even electrical vehicles by using the internet and advanced communication systems, which meets the flexibility of future relation between productions and consumptions [154]. This requires a cutting-edge research on planning economic dispatches, promoting optimal strategies and managing hierarchy of virtual power plants. Here the approaches based on integration of different energy systems, e.g. gas, heat, or electricity can play an important role in optimal exploitation of available generating and transmitting resources.

7.2. Discussions on future challenges

Firstly, the impacts of applying frequency response techniques on the lifetime of WTs are essential to power systems security. The International Electrotechnical Commission (IEC) standard states that the design lifetime of WTs is above 20 years [155]. In fact, some 28% of all installed WT capacity is currently older than 15 years [156]. In both [157,158], studies focus on the fatigue life of WTs. Reference [158] shows that blade's angle is more sensitive to the stress acting on blades, than chord length and the blade length considered in the study. Therefore, follow-up studies should consider the influences of fatigue life of each WTs' components on power performance.

Secondly, it is necessary to develop a new standard for evaluation of the stability of power systems. The electric frequency produced by synchronous generators is a critical indicator of the power system's health in the conventional power systems. However, in the future power systems that 100% dominated by inverter-interfaced RESs, it is not feasible for inverters to use a phase-locked loop to track the grid frequency. A core difference between a synchronous generator and an inverter-based generating source is that the former contains no moving parts. As mentioned, power electronics connected generation is generally characterised by having a zero inertia, and their response to the changes of the power system is determined by the control schemes implemented rather than the power imbalance.

Development of the next generation of *grid-forming inverters* must consider the compatibility of existing and future power systems and operability without participation of synchronous generators [14]. Virtual synchronous generator (VSG) is a control strategy that has been proposed to mitigate stability issues in RESs dominated power systems [159]. Compared to the traditional droop control, VSG can make RESs to deliver power as a dispatchable source. This is achieved by mimicking the inertial response characteristics of a synchronous generator [160]. Also, the rotating inertia can be emulated in grid-connected inverters, thus the rotating inertia is enhanced to ensure power system safety [161].

Thirdly, communication systems, currently used in a number of applications related to monitoring, control and protection [162–164], have a great prospect for improving the operation of modern power systems. Moreover, the load frequency control based on the sampled-data control is implemented to reduce the communication burden [165]. For a power system with reduced system inertia, the grid frequency is more likely to violate the statutory frequency limits due to the increased RoCoF. Moreover, measured frequency and corresponding RoCoF spread differently across the system. Therefore, if communication delays exceed a predefined level, it may result in the malfunction of in advanced created monitoring, control and protection functions relying on Information Communication Technology (ICT). To mitigate the foregoing problems, applications requiring only local information are designed in parallel to those based on wide area information. Meeting the UK carbon reduction targets requires a massive penetration of renewables. This will result in a reduced and

variable overall system inertia. Consequently, the speed of frequency decline for a given active power imbalance will increase, what might cause dangerous frequency instabilities. It follows that the development of a new, significantly faster, and optimised/coordinated frequency response solution using renewables, demand side resources, and other new technologies are becoming increasingly important. The UK *Enhanced Frequency Control Capability* (EFCC) project [162], led by National Grid ESO, was focused on development of a novel wide area frequency control scheme, capable of ensuring a stable system operation, also in scenarios with significantly increased percentage of the nonsynchronous generation. The project started in 2014 and finished in 2019. In general, the EFCC project was focused on the following vital challenges:

i)   Development of a wide area frequency control scheme to manage frequency response in a low inertia electricity system. This can provide a coordinated fast response to the power system.
ii)   Technical capability for faster frequency response from a range of service providers and their interfaces including communication protocols and site configurations.
iii)   Development of a novel EFCC (RoCoF-based) frequency response balancing service and its business model.
iv)   Demonstration of a fully centralized solution based on Linear Quadratic Gaussian Controller
v)   Assessment of solutions based on local information.

Any wide area control application has to be thoroughly tested before applied. Having in mind a large number of sensors and communication channels involved in such applications, serious hardware in the loop tasting facilities have to be implemented. Using RTDS testing facilities [166], the proposed EFCC solutions were thoroughly tested before demonstrated at the selected sites in the National Grid network. Furthermore, the local and wide-area smart frequency control based wide-area monitoring system supported by phasor measurement units is developed in [167] for low inertia power systems. The scheme is able to release fast, smart, coordinated and robust primary frequency response from different fast service providers like CCGT, wind units, photovoltaic, BESS and smart induction motors.

Next to the EFCC project, the recently accomplished Horizon 2020 MIGRATE project [168] was focused on future power systems with high penetration of inverter connected generation, the so-called nonsynchronous generation. In this context, one of the core project activities, directly related to frequency control, was monitoring of power system attributes directly affected by the increased penetration of nonsynchronous generation. In this context, novel approaches for monitoring of power system inertia were proposed [169–171]. One of particular research questions of the project was definition of regional inertia and approaches for its monitoring [170]. A number of effective approaches were developed and tested using field data, as well through a detailed real time digital simulation platform. The abovementioned approaches for inertia monitoring are based on the traditional swing equation describing synchronous generator dynamics. They are however based on the approach in which the system inertia can be determined after a large active power imbalance, provoking an evident frequency change. Here a precise frequency and RoCoF

measurement is a prerequisite for an accurate inertia determination.

As it is known, a trend of integrating different energy systems into a single one, e.g. integration of electricity, heat, or gas systems into a single one, is opening new opportunities for providing extra functionality of such as flexibility, resilience, optimal operation etc. From the perspective of the frequency stability, it is expected that future IESs will open mechanisms for supporting frequency stability and contributing to challenges related to decreased/variable power system inertia. New results in this area are expected in future.

8. Conclusions

This paper presents a comprehensive review of existing frequency response technologies for wind power-integrated energy systems. The control methods applied to wind turbines mainly fall under primary frequency control. As discussed, the existing control strategies highly depend on the operating point of wind turbines. In this context, two types of wind turbines control schemes, i.e., the temporary and persistent energy reserves, are fully detailed in the paper. The *temporary energy reserve* refers to the instantaneous release of kinetic energy stored in the rotating masses of wind turbines operating at maximum power point tracking. As discussed, this includes synthetic inertia control, droop control and fast energy reserve control. The de-loading control refers to the *persistent energy reserves* realised by pitch angle and rotor speed control. The frequency support is provided by making wind turbines operating at a suboptimal mode. In this review paper, i) the advantages/disadvantages of frequency control capabilities of wind units are discussed in terms of more practical aspects such as the form of energy and input signals required by these approaches, ii) the existing control approaches of arresting secondary frequency dips are reviewed for the first time and iii) the frequency control schemes developed within IESs are investigated. This paper sheds light on a wide variety of industrial and academic cases investigated by researchers/engineers, to date. It concludes that the level of the integration of renewable energy sources, communication infrastructure, system size and control strategies play a significant role in the quality of frequency response enhancement. In integrated energy systems, wind turbines cannot contribute to frequency response when wind speed is extremely low. Under such conditions, battery energy storage systems, energy conversion and other ancillary services would be viable options which can offer a minimum acceptable response and compensate for the power deficit caused by a frequency event. Therefore, by merging wind power, battery energy storage systems, and energy conversion solutions with frequency control methods within IESs is necessary to overcome high risks of blackouts caused by intermittent renewable energy sources. It is expected that many innovative control strategies emerge in a very short period of time as a result of technological enhancement and extensive ongoing research activities. The wide variety of challenges and emerging concepts addressed still require further in-depth studies. More attention ought to be paid to the improvements of existing frequency control schemes responding to generation disturbances. The impacts of these on the system behaviour under non-ideal conditions and well-established protection schemes need to be assessed. In brief, this paper provides

academic guidelines to researchers in the field and sheds light on the industrial progress made in updating some old-fashioned practices and technologies.

References

[1] Wu J, Yan J, Jia H, Hatziargyriou N, Djilali N, Sun H. Integrated energy systems. Appl Energy 2016;167:155–7. https://doi.org/10.1016/j.apenergy.2016.02.075.

[2] OECD (2016). World electricity generation by source of energy: Terawatt hours (TWh). Paris: OECD Publishing; 2016. https://doi.org/10.1787/factbook-2015-en.

[3] European Commission. The Road from Paris: assessing the implications of the Paris Agreement and accompanying the proposal for a Council decision on the signing, on behalf of the European Union, of the Paris agreement adopted under the United Nations Framework Convention on Cl. Commun from Comm to Eur Parliam Counc 2016;110:1–10.

[4] Holttinen H, Orths AG, Eriksen PB, Hidalgo J, Estanqueiro A, Groome F, et al. Currents of change. IEEE Power Energy Mag 2011;9:47–59. https://doi.org/10.1109/MPE.2011.942351.

[5] U.S. Energy Information Administration. Nuclear Power and the Environment n.d. https://www.eia.gov/energyexplained/index.php?page=nuclear_environment#.W4lnIewtd_Y.mendeley (accessed August 31, 2018).

[6] Pineda I, Pierre Tardieu W. Annual combined onshore and offshore wind energy statistics 2018. https://doi.org/10.1016/j.preghy.2016.08.046.

[7] Evans S. Analysis: UK renewables generate more electricity than fossil fuels for first time. 2019.

[8] Hu L, Xue F, Qin Z, Shi J, Qiao W, Yang W, et al. Sliding mode extremum seeking control based on improved invasive weed optimization for MPPT in wind energy conversion system. Appl Energy 2019;248:567–75. https://doi.org/10.1016/j.apenergy.2019.04.073.

[9] Kubik ML, Coker PJ, Barlow JF. Increasing thermal plant flexibility in a high renewables power system. Appl Energy 2015;154:102–11. https://doi.org/10.1016/j.apenergy.2015.04.063.

[10] Vidal-Amaro JJ, Østergaard PA, Sheinbaum-Pardo C. Optimal energy mix for transitioning from fossil fuels to renewable energy sources - The case of the Mexican electricity system. Appl Energy 2015;150:80–96. https://doi.org/10.1016/j.apenergy.2015.03.133.

[11] Zappa W, Junginger M, van den Broek M. Is a 100% renewable European power system feasible by 2050? Appl Energy 2019;233–234:1027–50. https://doi.org/10.1016/j.apenergy.2018.08.109.

[12] Malik A, Ravishankar J. A hybrid control approach for regulating frequency through demand response. Appl Energy 2018;210:1347–62. https://doi.org/10.1016/j.apenergy.2017.08.160.

[13] Kundur P. Power System Stability and Control. New York: Mc-Graw-Hill; 1994. https://doi.org/10.1287/orsc.1.2.177.

[14] Kroposki B, Johnson B, Zhang Y, Gevorgian V, Denholm P, Hodge BM, et al. Achieving a 100% Renewable Grid: Operating Electric Power Systems with Extremely High Levels of Variable Renewable Energy. IEEE Power Energy Mag 2017;15:819–26. https://doi.org/10.1109/MPE.2016.2637122.

[15] Australian Energy Market Operator (AEMO). Wind integration in electricity grids : International practice and experience 2011:1–50.

[16] Johnson SC, Rhodes JD, Webber ME. Understanding the impact of non-synchronous wind and solar generation on grid stability and identifying mitigation pathways. Appl Energy 2020;262:114492. https://doi.org/10.1016/j.apenergy.2020.114492.

[17] Arani MFM, El-Saadany EF. Implementing virtual inertia in DFIG-based wind power generation. IEEE Trans Power Syst 2013;28:1373–84. https://doi.org/10.1109/TPWRS.2012.2207972.

[18] National Gird. Enhanced frequency control capability (EFCC). 2014.

[19] Lopez S, Terzija V, Azizi S. Development and tests of new protection solutions when reaching 100 % PE penetration. EU H2020 MIGRATE Proj Deliv 43 2018.

[20] Miller N, Lew D, Piwko R. Technology capabilities for fast frequency response. 2017.

[21] Eto JH, Undrill J, Roberts C, Mackin P, Ellis J. Frequency control requirements for reliable interconnection frequency response 2018:1–116.

[22] Zhuo Z, Zhang N, Kang C, Dong R, Liu Y. Optimal operation of hybrid AC/DC distribution network with high penetrated renewable energy. IEEE Power Energy Soc Gen Meet 2018;2018-Augus:0–4. https://doi.org/10.1109/PESGM.2018.8585802.

[23] Temtem S, Creighton K, Cashman D, Skillen R. Summary of studies on rate of change of frequency events on the all-island system August 2012 2012:1–8.

[24] Prabha Kundur, Kundur P. Power system stability and control. 1994. https://doi.org/10.1016/S0022-3115(02)01404-6.

[25] Oliferovich N, Hryniuk D, Orobei I. Harmonic Identification of Technological Objects in Real Time. 2016 Open Conf Electr Electron Inf Sci 2016:1–4.

[26] Energy P, Road FS. Rate of change of frequency (RoCoF) review of TSO and generator submissions final report 2013.

[27] Lalor G, Ritchie J, Rourke S, Flynn D, O'Malley MJ. Dynamic frequency control with increasing wind generation. 2004 IEEE Power Eng. Soc. Gen. Meet., vol. 2, 2004, p. 1715–20. https://doi.org/10.1109/pes.2004.1373170.

[28] Terzija V V, Koglin H-J. Adaptive underfrequency load shedding integrated with a frequency estimation numerical algorithm. Gener Transm Distrib IEE Proc 2002;149:713–8.

[29] Terzija V V. Adaptive underfrequency load shedding based on the magnitude of the disturbance estimation. IEEE Trans Power Syst 2006;21:1260–6. https://doi.org/10.1109/TPWRS.2006.879315.

[30] Karimi M, Wall P, Mokhlis H, Terzija V. A new centralized adaptive underfrequency load shedding controller for microgrids based on a distribution state estimator. IEEE Trans Power Syst 2017;32:370–80.

[31] Li C, Wu Y, Sun Y, Zhang H, Liu Y, Member S, et al. Continuous under-frequency load shedding scheme for power system adaptive frequency control. IEEE Trans Power Syst 2020;35:950–61.

[32] Zhao J, Tang Y, Terzija V. Robust online estimation of power system center of inertia frequency. IEEE Trans Power Syst 2019;34:821–5.

[33] Quirós-Tortós J, Demetriou P, Panteli M, Kyriakides E, Terzija V. Intentional controlled islanding and risk assessment : A Uuified framework. IEEE Syst J 2018;12:3637–48.

[34] Ding L, Wall P, Terzija V. Graph spectra based controlled islanding for low inertia power systems. IEEE Trans Power Syst 2017;32:302–9. https://doi.org/10.1109/TPWRD.2016.2582519.

[35] Ding L, Guo Y, Wall P, Sun K, Member S, Terzija V. Identifying the timing of controlled islanding using a controlling UEP based method. IEEE Trans Power Syst 2018;33:5913–22. https://doi.org/10.1109/TPWRS.2018.2842709.

[36] Ding L, Gonzalez-longatt FM, Member S, Wall P, Terzija V, Member S. Two-step spectral clustering controlled islanding algorithm. IEEE Trans Power Syst 2013;28:75–84.

[37] Lie X, Cartwright P. Direct active and reactive power control of DFIG for wind energy generation. IEEE Trans Energy Convers 2006;21:750–8. https://doi.org/10.1109/TEC.2006.875472.

[38] Mauricio JM, Marano A, Gomez-Exposito A, Martinez Ramos JL. Frequency regulation contribution through variable-speed wind energy conversion systems. IEEE Trans Power Syst 2009;24:173–80. https://doi.org/10.1109/TPWRS.2008.2009398.

[39] J.G. Slootweg * WLK, Electrical. The impact of large scale wind power generation on power system oscillations. Electr Power Syst Res 2003;67:9–20. https://doi.org/10.1016/S0378-7796(03)00089-0.

[40] Pannell G, Atkinson DJ, Zahawi B. Minimum-threshold crowbar for a fault-ride-through grid-code-compliant DFIG wind turbine. IEEE Trans Energy Convers 2010;25:750–9. https://doi.org/10.1109/TEC.2010.2046492.

[41] The Switch. PMG vs . DFIG – the big generator technology debate 2014:1–6. https://theswitch.com/download-center/talking-points/wind/pmg-vs-dfig-the-big-generator-technology-debate/.

[42] Lu Z, Ye Y, Qiao Y. An adaptive frequency regulation method with grid-friendly restoration for VSC-HVDC integrated offshore wind farms. IEEE Trans Power Syst 2019;34:3582–93. https://doi.org/10.1109/tpwrs.2019.2901986.

[43] Huang C, Li F, Jin Z. Maximum power point tracking strategy for

large-scale wind generation systems considering wind turbine dynamics. IEEE Trans Ind Electron 2015;62:2530–9. https://doi.org/10.1109/TIE.2015.2395384.

[44] Itani S El, Annakkage UD, Joos G. Short-term frequency support utilizing inertial response of DFIG wind turbines. IEEE Power Energy Soc Gen Meet 2011:1–8. https://doi.org/10.1109/PES.2011.6038914.

[45] Rodr MA, Lo J, Marroyo L, Engineers E. Introduction to a wind energy generation system. Doubly Fed Induction Mach. Model. Control Wind Energy Gener., 2011, p. 1–85. https://doi.org/10.1002/9781118104965.ch1.

[46] Fu Y, Zhang X, Hei Y, Wang H. Active participation of variable speed wind turbine in inertial and primary frequency regulations. Electr Power Syst Res 2017;147:174–84. https://doi.org/10.1016/j.epsr.2017.03.001.

[47] Wu Z, Gao W, Wang X, Kang M, Hwang M, Kang YC, et al. Improved inertial control for permanent magnet synchronous generator wind turbine generators. IET Renew Power Gener 2016;10:1366–73. https://doi.org/10.1049/iet-rpg.2016.0125.

[48] Yin M, Yang Z, Xu Y, Liu J, Zhou L, Zou Y. Aerodynamic optimization for variable-speed wind turbines based on wind energy capture efficiency. Appl Energy 2018;221:508–21. https://doi.org/10.1016/j.apenergy.2018.03.078.

[49] González LG, Figueres E, Garcerá G, Carranza O. Maximum-power-point tracking with reduced mechanical stress applied to wind-energy-conversion-systems. Appl Energy 2010;87:2304–12. https://doi.org/10.1016/j.apenergy.2009.11.030.

[50] Fathabadi H. Novel high-efficient unified maximum power point tracking controller for hybrid fuel cell/wind systems. Appl Energy 2016;183:1498–510. https://doi.org/10.1016/j.apenergy.2016.09.114.

[51] Song D, Fan X, Yang J, Liu A, Chen S, Joo YH. Power extraction efficiency optimization of horizontal-axis wind turbines through optimizing control parameters of yaw control systems using an intelligent method. Appl Energy 2018;224:267–79. https://doi.org/10.1016/j.apenergy.2018.04.114.

[52] Dreidy M, Mokhlis H, Mekhilef S. Inertia response and frequency control techniques for renewable energy sources: A review. Renew Sustain Energy Rev 2017;69:144–55. https://doi.org/10.1016/j.rser.2016.11.170.

[53] Eriksson R, Modig N, Elkington K. Synthetic inertia versus fast frequency response: a definition. IET Renew Power Gener 2017;12:507–14. https://doi.org/10.1049/iet-rpg.2017.0370.

[54] F. Gonzalez-Longatt. Impact of synthetic inertia from wind power on the protection / control schemes of future power systems : Simulation study. 11th IET Int Conf Dev Power Syst Prot (DPSP 2012) 2012.

[55] Gonzalez-Longatt F, Chikuni E, Rashayi E. Effects of the Synthetic Inertia from wind power on the total system inertia after a frequency disturbance. Proc IEEE Int Conf Ind Technol 2013:826–32. https://doi.org/10.1109/ICIT.2013.6505779.

[56] Pudjianto D, Pudjianto D, Ramsay C, Ramsay C, Strbac G, Strbac G. Frequency support from doubly fed induction generator wind turbines. Renew Power Gener IET 2007;1:10–16. https://doi.org/10.1049/iet-rpg.

[57] Dharmawardena H, Uhlen K, Gjerde SS. Modelling wind farm with synthetic inertia for power system dynamic studies. 2016 IEEE Int Energy Conf 2016:1–6. https://doi.org/10.1109/ENERGYCON.2016.7514098.

[58] Wang Z, Wu W. Coordinated Control Method for DFIG-Based Wind Farm to Provide Primary Frequency Regulation Service. IEEE Trans Power Syst 2017;33:1–1. https://doi.org/10.1109/TPWRS.2017.2755685.

[59] Morren J, de Haan SWH, Kling WL, Ferreira JA. Wind turbines emulating inertia and supporting primary frequency control. IEEE Trans Power Syst 2006;21:433–4. https://doi.org/10.1109/TPWRS.2005.861956.

[60] Rahmann C, Jara J, Salles MBC. Effects of inertia emulation in modern wind parks on isolated power systems. IEEE Power Energy Soc Gen Meet 2015;2015-Septe:1–5. https://doi.org/10.1109/PESGM.2015.7285749.

[61] Nguyen HT, Yang G, Nielsen AH, Jensen PH. Frequency stability enhancement for low inertia systems using synthetic inertia of wind power 2017:2–5.

[62] Terzija V, Djuric M. Direct estimation of voltage phasor, frequency and its rate of change using Newton's iterative method. Int J Electr Power Energy Syst 1994;16:423–8. https://doi.org/10.1016/0142-0615(94)90030-2.

[63] Djurić MB, Terzija V V. An algorithm for frequency relaying based on the Newton-Raphson method. Electr Power Syst Res 1994;31:119–24. https://doi.org/10.1016/0378-7796(94)90089-2.

[64] Terzija V, Djurić MB, Jeremić NŽ. A recursive Newton type algorithm for digital frequency relaying. Electr Power Syst Res 1996;36:67–72.

[65] Terzija V V., Djuric MB, Kovacevic BD. Voltage phasor and local system frequency estimation using newton type algorithm. IEEE Trans Power Deliv 1994;9:1368–74. https://doi.org/10.1109/61.311162.

[66] Terzija V V. Improved recursive Newton-type algorithm for frequency and spectra estimation in power systems. IEEE Trans Instrum Meas 2003;52:1654–9. https://doi.org/10.1109/TIM.2003.817152.

[67] European commission. Commission Regulation (EU) 2016/631 Establishing a network code on requirements for grid connection of generators. Off J Eur Union 2016:68. https://doi.org/10.1017/CBO9781107415324.004.

[68] Zhang Z-S, Sun Y-Z, Lin J, Li G-J. Coordinated frequency regulation by doubly fed induction generator-based wind power plants. IET Renew Power Gener 2012;6:38. https://doi.org/10.1049/iet-rpg.2010.0208.

[69] Tan Y, Member S, Meegahapola L, Muttaqi KM, Member S. A suboptimal power-point-tracking-based primary frequency response strategy for DFIGs in hybrid remote area power supply systems. IEEE Trans Energy Convers 2015;31:1–13. https://doi.org/10.1109/TEC.2015.2476827.

[70] Díaz-González F, Hau M, Sumper A, Gomis-Bellmunt O. Participation of wind power plants in system frequency control: Review of grid code requirements and control methods. Renew Sustain Energy Rev 2014;34:551–64. https://doi.org/10.1016/j.rser.2014.03.040.

[71] Sun Y, Zhang Z, Li G, Lin J. Review on frequency control of power systems with wind power penetration. 2010 Int Conf Power Syst Technol 2010:1–8. https://doi.org/10.1109/POWERCON.2010.5666151.

[72] Verbič G, Member S, Hill DJ. Frequency support from wind turbine generators with a time-variable droop characteristic. IEEE Trans Sustain ENERGY 2018;9:676–84.

[73] Van de Vyver J, De Kooning JDMM, Meersman B, Vandevelde L, Vandoorn TL. Droop control as an alternative inertial response strategy for the synthetic inertia on wind turbines. IEEE Trans Power Syst 2016;31:1129–38. https://doi.org/10.1109/TPWRS.2015.2417758.

[74] Conroy JF, Watson R. Frequency response capability of full converter wind turbine generators in comparison to conventional generation. IEEE Trans Power Syst 2008;23:649–56. https://doi.org/10.1109/TPWRS.2008.920197.

[75] Zhang Y, Ooi BT. Stand-Alone doubly-fed induction generators (DFIGs) with autonomous frequency control. IEEE Trans Power Deliv 2013;28:752–60. https://doi.org/10.1109/TPWRD.2013.2243170.

[76] Hwang M, Muljadi E, Park J-W, Sørensen P, Kang YC. Dynamic droop–based inertial control of a doubly-fed induction generator. IEEE Trans Sustain ENERGY 2016;7:2971–9.

[77] Hwang M, Muljadi E, Jang G, Kang YC. Disturbance-adaptive short-term frequency support of a DFIG associated with the variable gain based on the RoCoF and rotor speed. IEEE Trans Power Syst 2017;32:1873–81. https://doi.org/10.1109/TPWRS.2016.2592535.

[78] Wilches-Bernal F, Chow JH, Sanchez-Gasca JJ. A fundamental study of applying wind turbines for power system frequency control. IEEE Trans Power Syst 2016;31:1496–505. https://doi.org/10.1109/TPWRS.2015.2433932.

[79] Zhang X, Zha X, Yue S, Chen Y. A frequency regulation strategy for wind power based on limited over-speed de-loading curve partitioning. IEEE Access 2018;6:22938–51. https://doi.org/10.1109/ACCESS.2018.2825363.

[80] Tarnowski GC, Kjær PC, Sørensen PE, Østergaard J. Variable speed wind turbines capability for frequency response. EWEC 2009 Sci Proc 2009:190–3.

[81] Lee J, Jang G, Muljadi E, Blaabjerg F, Chen Z, Cheol Kang Y. Stable short-term frequency support using adaptive gains for a DFIG-based wind power plant. IEEE Trans Energy Convers 2016;31:1068–179. https://doi.org/10.1109/TEC.2016.2532366.

[82] Hong DY, Ji TY, Li MS, Wu QH. Ultra-short-term forecast of wind speed and wind power based on morphological high frequency filter and double similarity search algorithm. Int J

Electr Power Energy Syst 2019;104:868–79.
https://doi.org/10.1016/j.ijepes.2018.07.061.

[83] Li L, Li Y, Zhou B, Wu Q, Shen X, Liu H, et al. An adaptive time-resolution method for ultra-short-term wind power prediction. Int J Electr Power Energy Syst 2020;118:105814. https://doi.org/10.1016/j.ijepes.2019.105814.

[84] Lin Z, Liu X, Collu M. Wind power prediction based on high-frequency SCADA data along with isolation forest and deep learning neural networks. Int J Electr Power Energy Syst 2020;118:105835. https://doi.org/10.1016/j.ijepes.2020.105835.

[85] De Prada Gil M, Gomis-Bellmunt O, Sumper A. Technical and economic assessment of offshore wind power plants based on variable frequency operation of clusters with a single power converter. Appl Energy 2014;125:218–29. https://doi.org/10.1016/j.apenergy.2014.03.031.

[86] Gao X, Li B, Wang T, Sun H, Yang H, Li Y, et al. Investigation and validation of 3D wake model for horizontal-axis wind turbines based on filed measurements. Appl Energy 2020;260. https://doi.org/10.1016/j.apenergy.2019.114272.

[87] Katic, I., Hojstrup, J., Jensen NO. A simple model for cluster efficiency. Eur. Wind energy Assoc., 1986, p. 407–10.

[88] Grassi S, Junghans S, Raubal M. Assessment of the wake effect on the energy production of onshore wind farms using GIS. Appl Energy 2014;136:827–37. https://doi.org/10.1016/j.apenergy.2014.05.066.

[89] Abraham A, Hong J. Dynamic wake modulation induced by utility-scale wind turbine operation. Appl Energy 2020;257:114003. https://doi.org/10.1016/j.apenergy.2019.114003.

[90] Gao X, Wang T, Li B, Sun H, Yang H, Han Z, et al. Investigation of wind turbine performance coupling wake and topography effects based on LiDAR measurements and SCADA data. Appl Energy 2019;255:113816. https://doi.org/10.1016/j.apenergy.2019.113816.

[91] Brogna R, Feng J, Sørensen JN, Shen WZ, Porté-Agel F. A new wake model and comparison of eight algorithms for layout optimization of wind farms in complex terrain. Appl Energy 2019;259:114189. https://doi.org/10.1016/j.apenergy.2019.114189.

[92] Xu J, Chen Y, Liao S, Sun Y, Yao L, Fu H, et al. Demand side industrial load control for local utilization of wind power in isolated grids. Appl Energy 2019;243:47–56. https://doi.org/10.1016/j.apenergy.2019.03.039.

[93] González-Longatt F, Wall PP, Terzija V. Wake effect in wind farm performance: Steady-state and dynamic behavior. Renew Energy 2012;39:329–38. https://doi.org/10.1016/j.renene.2011.08.053.

[94] Vidyanandan K V., Senroy N. Primary frequency regulation by deloaded wind turbines using variable droop. IEEE Trans Power Syst 2013;28:837–46. https://doi.org/10.1109/TPWRS.2012.2208233.

[95] Ackermann T. Wind Power in Power Systems. vol. 8. 2005. https://doi.org/10.1002/0470012684.

[96] Jin Y, Ju P, Rehtanz C, Wu F, Pan X. Equivalent modeling of wind energy conversion considering overall effect of pitch angle controllers in wind farm. Appl Energy 2018;222:485–96. https://doi.org/10.1016/j.apenergy.2018.03.180.

[97] Xu YL, Peng YX, Zhan S. Optimal blade pitch function and control device for high-solidity straight-bladed vertical axis wind turbines. Appl Energy 2019;242:1613–25. https://doi.org/10.1016/j.apenergy.2019.03.151.

[98] de Almeida RG, Castronuovo ED, Peças Lopes JA. Optimum generation control in wind parks when carrying out system operator requests. IEEE Trans Power Syst 2006;21:718–25. https://doi.org/10.1109/TPWRS.2005.861996.

[99] Ghosh S, Senroy N. Electromechanical dynamics of controlled variable-speed wind turbines. IEEE Syst J 2015;9:639–46. https://doi.org/10.1109/JSYST.2013.2280037.

[100] Yuan X, Li Y. Control of variable pitch and variable speed direct-drive wind turbines in weak grid systems with active power balance. IET Renew Power Gener 2014;8:119–31. https://doi.org/10.1049/iet-rpg.2012.0212.

[101] Naik KA, Gupta CP. Fuzzy logic based pitch angle controller for SCIG based wind energy system. 2017 Recent Dev. Control. Auto mation Power Eng., vol. 3, n.d., p. 1–6.

[102] Palejiya D, Chen D. Performance improvements of switching control for wind turbines. IEEE Trans Sustain Energy 2016;7:526–34. https://doi.org/10.1109/TSTE.2015.2502262.

[103] Barklund E, Pogaku N, Prodanovic M, Hernandez-Aramburo C, Green TC. Energy management in autonomous microgrid using stability-constrained droop control of inverters. IEEE Trans Power Electron 2008;23:2346–52. https://doi.org/10.1109/TPEL.2008.2001910.

[104] Margaris ID, Papathanassiou SA, Hatziargyriou ND, Hansen AD, Sorensen P. Frequency control in autonomous power systems with high wind power penetration. IEEE Trans Sustain Energy 2012;3:189–99. https://doi.org/10.1109/TSTE.2011.2174660.

[105] Luo H, Hu Z, Zhang H, Chen H. Coordinated Active Power Control Strategy for Deloaded Wind Turbines to Improve Regulation Performance in AGC. IEEE Trans Power Syst 2018;PP:1. https://doi.org/10.1109/TPWRS.2018.2867232.

[106] Arani MFM, Mohamed YARI. Analysis and mitigation of undesirable impacts of implementing frequency support controllers in wind power generation. IEEE Trans Energy Convers 2016;31:174–86. https://doi.org/10.1109/TEC.2015.2484380.

[107] De Rijcke S, Tielens P, Rawn B, Van Hertem D, Driesen J. Trading energy yield for frequency regulation: optimal control of kinetic energy in wind farms. IEEE Trans Power Syst 2015;30:2469–78. https://doi.org/10.1109/TPWRS.2014.2357684.

[108] Fu Y, Wang Y, Zhang X. Integrated wind turbine controller with virtual inertia and primary frequency responses for grid dynamic frequency support. IET Renew Power Gener 2017;11:1129–37. https://doi.org/10.1049/iet-rpg.2016.0465.

[109] Arani MFM, Mohamed YA-RI. Dynamic Droop Control for Wind Turbines Participating in Primary Frequency Regulation in Microgrids. IEEE Trans Smart Grid 2017;9:1–1. https://doi.org/10.1109/TSG.2017.2696339.

[110] Azizipanah-abarghooee R, Malekpour M, Blaabjerg F, Terzija V. A linear inertial response emulation for variable speed wind turbines. IEEE Trans Power Syst 2020;35:1198–208.

[111] Kang M, Lee J, Kang YC. Modified stepwise inertial control using the mechanical input and electrical output curves of a doubly fed induction generator. 9th Int Conf Power Electron - ECCE Asia "Green World with Power Electron ICPE 2015-ECCE Asia 2015:357–61. https://doi.org/10.1109/ICPE.2015.7167810.

[112] Bao W, Ding L, Yin S, Wang K, Terzija V. Active rotor speed protection for DFIG synthetic inertia control. IET Conf Publ 2016;2016:1–5.

[113] Liu Z, Ding L, Wang K, Ma Z, Bao W, Liu Q. Control strategy to mitigate secondary frequency dips for DFIG with virtual inertial control. China Int Conf Electr Distrib CICED 2016;2016-Septe:10–3. https://doi.org/10.1109/CICED.2016.7576211.

[114] Liu K, Qu Y, Kim HM, Song H. Avoiding frequency second dip in power unreserved control during wind power rotational speed recovery. IEEE Trans Power Syst 2018;33:3097–106. https://doi.org/10.1109/TPWRS.2017.2761897.

[115] Kang M, Kim K, Muljadi E, Park JW, Kang YC. Frequency control support of a doubly-fed induction generator based on the torque limit. IEEE Trans Power Syst 2016;31:4575–83. https://doi.org/10.1109/TPWRS.2015.2514240.

[116] Kang M, Muljadi E, Hur K, Kang YC. Stable adaptive inertial control of a doubly-fed induction generator. IEEE Trans Smart Grid 2016;7:2971–9. https://doi.org/10.1109/TSG.2016.2559506.

[117] Sun K, Xiao H, You S, Li H, Pan J, Li KJ, et al. Frequency secure control strategy for power grid with large-scale wind farms through HVDC links. Int J Electr Power Energy Syst 2020;117:105706. https://doi.org/10.1016/j.ijepes.2019.105706.

[118] Bao W, Ding L, Liu Z, Zhu G, Kheshti M, Wu Q, et al. Analytically derived fixed termination time for stepwise inertial control of wind turbines Part I: Analytical derivation. IET Renew Power Gen 2020;121:106120. https://doi.org/10.1016/j.ijepes.2020.106120.

[119] Guo Y, Bao W, Ding L, Liu Z, Kheshti M, Wu Q, et al. Analytically derived fixed termination time for stepwise inertial control of wind turbines—Part II: Application strategy. Int J Electr Power Energy Syst 2020;121:106106. https://doi.org/10.1016/j.ijepes.2020.106106.

[120] Meegahapola LG, Flynn D. Investigation of frequency stability during high penetration of CCGTs and variable-speed wind generators in electricity networks. IEEE Power Energy Soc. Gen. Meet., vol. 2015- Septe, IEEE; 2015, p. 1–5. https://doi.org/10.1109/PESGM.2015.7286176.

[121] Saha D, Saikia LC. Automatic generation control of an

17

interconnected CCGT - thermal system using stochastic fractal search optimized classical controllers. Int Trans Electr Energy Syst 2018:1–25. https://doi.org/10.1002/etep.2533.

[122] Saha D, Saikia LC. Impact of phase-locked loop on system dynamics of a CCGT incorporated diverse source system employed with AC / DC interconnection. J Renew Sustain Energy 2018;045506. https://doi.org/10.1063/1.5000254.

[123] Saha A, Saikia LC. Renewable energy source - based multiarea AGC system with integration of EV utilizing cascade controller considering time delay. Int Trans Electr Energy Syst 2019:1–22. https://doi.org/10.1002/etep.2646.

[124] Du P, Li W. Frequency response impact of integration of HVDC into a low-inertia AC power grid. IEEE Trans Power Syst 2020;8950:1–1. https://doi.org/10.1109/tpwrs.2020.2990304.

[125] Junyent-Ferré A, Pipelzadeh Y, Green TC. Blending HVDC-link energy storage and offshore wind turbine inertia for fast frequency response. IEEE Trans Sustain Energy 2015;6:1059–66. https://doi.org/10.1109/TSTE.2014.2360147.

[126] Liu H, Chen Z. Contribution of VSC-HVDC to frequency regulation of power systems with offshore wind generation. IEEE Trans Energy Convers 2015;30:918–26. https://doi.org/10.1109/TEC.2015.2417130.

[127] Conlon T, Waite M, Modi V. Assessing new transmission and energy storage in achieving increasing renewable generation targets in a regional grid. Appl Energy 2019;250:1085–98. https://doi.org/10.1016/j.apenergy.2019.05.066.

[128] Melo SP, Brand U, Vogt T, Telle JS, Schuldt F, Maydell K V. Primary frequency control provided by hybrid battery storage and power-to-heat system. Appl Energy 2019;233–234:220–31. https://doi.org/10.1016/j.apenergy.2018.09.177.

[129] Sowa T, Krengel S, Koopmann S, Nowak J. Multi-criteria operation strategies of power-to-heat-Systems in virtual power plants with a high penetration of renewable energies. Energy Procedia 2014;46:237–45. https://doi.org/10.1016/j.egypro.2014.01.178.

[130] Xu X, Ming W, Zhou Y, Wu J. Coordinative control of CHP generation and battery for frequency response. IEEE Power Energy Soc Gen Meet 2019;2019-Augus. https://doi.org/10.1109/PESGM40551.2019.8973982.

[131] Strunck C, Albrecht M, Rehtanz C. Provision of ancillary services by different decentralized energy resources. 2019 IEEE Milan PowerTech, PowerTech 2019 2019:3–8. https://doi.org/10.1109/PTC.2019.8810646.

[132] Qin X, Zhang X, Shen X, Xu Y, Shahidehpour M, Sun H. Distributed optimal frequency control for integrated energy systems with electricity and heat. IEEE Power Energy Soc Gen Meet 2019;2019-Augus:11–5. https://doi.org/10.1109/PESGM40551.2019.8973847.

[133] D NL, Vasquez JC, Member S, Guerrero JM. A communication-less distributed control architecture for islanded microgrids with renewable generation and storage. IEEE Trans Power Electron 2018;33:1922–39.

[134] Kim M, Kwasinski A. Decentralized hierarchical control of active power distribution nodes. IEEE Trans Energy Convers 2014;29:934–43.

[135] Latif A, Hussain SMS, Das DC, Ustun TS. State-of-the-art of controllers and soft computing techniques for regulated load frequency management of single/multi-area traditional and renewable energy based power systems. Appl Energy 2020;266:114858. https://doi.org/10.1016/j.apenergy.2020.114858.

[136] Shiroei M, Ranjbar AM. Electrical power and energy systems supervisory predictive control of power system load frequency control. Int J Electr Power Energy Syst 2014;61:70–80. https://doi.org/10.1016/j.ijepes.2014.03.020.

[137] Patsalides M, Papadimitriou CN, Efthymiou V, Ciavarella R, Somma M Di, Wakszyńska A, et al. Frequency stability evaluation in low inertia systems utilizing smart hierarchical controllers. Energies 2020;13. https://doi.org/10.3390/en13133506.

[138] Ciavarella R, Graditi G, Valenti M, Strasser TI. Innovative frequency controls for intelligent power systems. Int. Symp. Power Electron. Electr. Drives, Autom. Motion, 2018, p. 656–60.

[139] Gao Y, Ai Q. Hierarchical coordination control for interconnected operation of electric-thermal-gas integrated energy system with micro-energy internet clusters. IEEE J Emerg Sel Top Power Electron 2018;6777. https://doi.org/10.1109/JESTPE.2018.2838144.

[140] Wu YK, Yang WH, Hu YL, Dzung PQ. Frequency regulation at a wind farm using time-varying inertia and droop controls. IEEE Trans Ind Appl 2019;55:213–24. https://doi.org/10.1109/TIA.2018.2868644.

[141] Wang Z, Wu W. Coordinated control method for DFIG-based wind farm to provide primary frequency regulation service. IEEE Trans Power Syst 2018;33:2644–59. https://doi.org/10.1109/TPWRS.2017.2755685.

[142] Lee J, Muljadi E, Sørensen P, Kang YC. Releasable kinetic energy-based inertial control of a DFIG wind power plant. IEEE Trans Sustain Energy 2016;7:279–88. https://doi.org/10.1109/TSTE.2015.2493165.

[143] Hou P, Hu W, Soltani M, Chen C, Zhang B, Chen Z. Offshore wind farm layout design considering optimized power dispatch strategy. IEEE Trans Sustain Energy 2017;8:638–47. https://doi.org/10.1109/TSTE.2016.2614266.

[144] Sun J, Li M, Zhang Z, Xu T, He J, Wang H, et al. Renewable energy transmission by HVDC across the continent: system challenges and opportunities. CSEE J Power Energy Syst 2017;3:353–64. https://doi.org/10.17775/cseejpes.2017.01200.

[145] Buchhagen C, Rauscher C, Menze A, Jung J. BorWin1 - First experiences with harmonic interactions in converter dominated grids. Proc. Int. ETG Congr. 2015, 2015, p. 27–33.

[146] Buchhagen C, Greve M, Menze A, Jung J. Harmonic stability - practical experience of a TSO. Proc. 15th Wind Integr Work, 2016, p. 1–6.

[147] Liu G, Azizi S, Sun M, Popov M, Terzija V. Performance of out-of-step tripping protection under renewable integration. J Eng 2018;2018:1216–22. https://doi.org/10.1049/joe.2018.0180.

[148] Shu Z, Jirutitijaroen P. Optimal operation strategy of energy storage system for grid-connected wind power plants. IEEE Trans Sustain Energy 2014;5:190–9. https://doi.org/10.1109/TSTE.2013.2278406.

[149] Cao J, Du W, Wang H, McCulloch M. Optimal sizing and control strategies for hybrid storage system as limited by grid frequency deviations. IEEE Trans Power Syst 2018;33:5486–95. https://doi.org/10.1109/TPWRS.2018.2805380.

[150] Dui X, Zhu G, Yao L. Two-stage optimization of battery energy storage capacity to decrease wind power curtailment in grid-connected wind farms. IEEE Trans Power Syst 2018;33:3296–305. https://doi.org/10.1109/TPWRS.2017.2779134.

[151] Tan Y, Muttaqi KM, Ciufo P, Meegahapola L, Guo X, Chen B, et al. Enhanced frequency regulation using multilevel energy storage in remote area power supply systems. IEEE Trans Power Syst 2019;34:163–70. https://doi.org/10.1109/TPWRS.2018.2867190.

[152] Etherden N, Vyatkin V, Bollen MHJ. Virtual power plant for grid services using IEC 61850. IEEE Trans Ind Informatics 2016;12:437–47. https://doi.org/10.1109/TII.2015.2414354.

[153] Koraki D, Strunz K. Wind and solar power integration in electricity markets and distribution networks through service-centric virtual power plants. IEEE Trans Power Syst 2018;33:473–85. https://doi.org/10.1109/TPWRS.2017.2710481.

[154] Yang Q, Yang T, Li W, editors. Smart power distribution systems: Control, Communication, and Optimization. 2019. https://doi.org/https://doi.org/10.1016/C2016-0-03261-8.

[155] Ziegler L, Gonzalez E, Rubert T, Smolka U, Melero JJ. Lifetime extension of onshore wind turbines: A review covering Germany, Spain, Denmark, and the UK. Renew Sustain Energy Rev 2018;82:1261–71. https://doi.org/10.1016/j.rser.2017.09.100.

[156] Giorgio Corbetta & Thomas Miloradovic. Wind in power. EWEA Eropean Stat 2016:1–12. https://doi.org/10.1186/1754-1611-7-28.

[157] Rezaeiha A, Kalkman I, Blocken B. Effect of pitch angle on power performance and aerodynamics of a vertical axis wind turbine. Appl Energy 2017;197:132–50. https://doi.org/10.1016/j.apenergy.2017.03.128.

[158] Tawade S V., Todkar SB, Hade AS. Fatigue life optimization of wind turbine blade. Int J Res Eng Technol 2014:843–50.

[159] Zhong QC, Weiss G. Synchronverters: Inverters that mimic synchronous generators. IEEE Trans Ind Electron 2011;58:1259–67. https://doi.org/10.1109/TIE.2010.2048839.

[160] Liu J, Miura Y, Ise T. Comparison of Dynamic Characteristics between Virtual Synchronous Generator and Droop Control in Inverter-Based Distributed Generators. IEEE Trans Power Electron 2016;31:3600–11. https://doi.org/10.1109/TPEL.2015.2465852.

[161] Wang F, Zhang L, Feng X, Guo H. An adaptive control strategy for virtual synchronous generator. IEEE Trans Ind Appl

2018;54:5124–33. https://doi.org/10.1109/TIA.2018.2859384.

[162]   Cai D, Wall P, Osborne M, Terzija V. Roadmap for the deployment of WAMPAC in the future GB power system. IET Gener Transm Distrib 2016;10:1553–62. https://doi.org/10.1049/iet-gtd.2015.0582.

[163]   Cai D, Regulski P, Osborne M, Terzija V. Wide area inter-area oscillation monitoring using fast nonlinear estimation algorithm. IEEE Trans Smart Grid 2013;4:1721–31. https://doi.org/10.1109/TSG.2013.2257890.

[164]   Terzija V, Valverde G, Cai D, Regulski P, Madani V, Fitch J, et al. Wide-area monitoring, protection, and control of future electric power networks. Proc IEEE 2011;99:80–93. https://doi.org/10.1109/JPROC.2010.2060450.

[165]   Shang-Guan X, He Y, Zhang C, Jiang L, Spencer JW, Wu M. Sampled-data based discrete and fast load frequency control for power systems with wind power. Appl Energy 2020;259:114202. https://doi.org/10.1016/j.apenergy.2019.114202.

[166]   RTDS Technologies n.d. https://www.rtds.com/ (accessed June 20, 2020).

[167]   Azizipanah-abarghooee R. Wide - Area Monitoring based Smart Frequency Control in Future Low - Variable Inertia Systems with CCGT / Wind / PV / BES / Load. University of Manchester, 2018.

[168]   Wilson D, Terzija V, Yu J, Nechifor A, Eves M. Deliverable 2.1 requirements for monitoring & forecasting PE-based KPIs. 2018.

[169]   Sun M, Feng Y, Wall P, Azizi S, Yu J, Terzija V. On-line power system inertia calculation using wide area measurements. Int J Electr Power Energy Syst 2019;109:325–31. https://doi.org/10.1016/j.ijepes.2019.02.013.

[170]   Wilson D, Yu J, Al-Ashwal N, Heimisson B, Terzija V. Measuring effective area inertia to determine fast-acting frequency response requirements. Int J Electr Power Energy Syst 2019;113:1–8. https://doi.org/10.1016/j.ijepes.2019.05.034.

[171]   Wall P, Terzija V. Simultaneous estimation of the time of disturbance and inertia in power systems. IEEE Trans Power Deliv 2014;29:2018–31. https://doi.org/10.1109/TPWRD.2014.2306062.